NBS-GCR-87-534

Transient Cooling of a Hot Surface by Droplets Evaporation

M. di Marzo, Z.Y. Wang and W.H. Meng

November 1987

Sponsored by:
U.S. DEPARTMENT OF COMMERCE
National Bureau of Standards
Center for Fire Research
Gaithersburg, MD 20899

NBS-GCR-87-534

TRANSIENT COOLING OF A HOT SURFACE BY DROPLETS EVAPORATION

M. di Marzo, Z.Y. Wang and W.H. Meng

University of Maryland
Mechanical Engineering Dept.
College Park, MD 20742

November 1987

Grant Number 70NANB5HO525

Sponsored by:
U.S. DEPARTMENT OF COMMERCE
National Bureau of Standards
Center for Fire Research
Gaithersburg, MD 20899

Notice

This report was prepared for the Center for Fire Research of the National Engineering Laboratory, National Bureau of Standards under Grant Number 70NANB5H0525. The statements and conclusions contained in this report are those of the authors and do not necessarily reflect the views of the National Bureau of Standards or the Center for Fire Research.

TRANSIENT COOLING OF A HOT SURFACE BY DROPLETS EVAPORATION

Final Report

M. di Marzo, Z. Y. Wang, W. H. Meng

Prepared for the

Center for Fire Research

National Bureau of Standards

Gaithersburg, MD 20899

Mechanical Engineering Department

Report No. 87-11

University of Maryland

College Park, Md 20742

August 1987

ABSTRACT

This report describes the research performed during the period March 1986 - March 1987 under a joint research program between the Mechanical Engineering Department of the University of Maryland and the Center for Fire Research of the National Bureau of Standards. The research is conducted in the laboratories of the CFR by a Graduate Research Assistant of the ME Department under the joint supervision of Dr. Marino di Marzo (ME Dept.-UMCP) and of Dr. David D. Evans (CFR - NBS).

The study of droplet evaporation on a high thermal conductivity semi-infinite solid is investigated as well as the solid thermal behavior both theoretically and experimentally. The behavior of a low thermal conductivity solid is the objective of experimental studies. A coupled analytical model for the solid and the evaporating liquid is being derived to predict the cooling effect induced by the evaporating droplet. The results of the analytical model will be available in the Summer 1987.

In parallel with the single droplet study, a preliminary modelling effort is initiated to characterize the cooling effect of a multi-droplet array. Typical spray distributions are used to derive some information on overall cooling effect of a hot surface.

A summary of the presentations and of the publications produced during the reporting period is also enclosed. A brief outline of the future research activities is given in the end of this report to provide a (prospective) of the reported results in the framework of the overall research program.

TABLE OF CONTENT

1. INTRODUCTION

1.1 Background 5

1.2 Overview 6

1.3 Program Development 7

2. EXPERIMENTAL MEASUREMENTS

2.1 Deposition Technique 9

2.2 Experimental Procedures 13

2.3 Experiments With Glass 14

2.4 Experiments With Macor 15

2.5 Data Collection 15

3. THEORETICAL MODEL

3.1 Theoretical Approach 28

3.2 Numerical Methods 33

3.3 Nomenclature 34

4. MULTI-DROPLET MODEL

4.1 Problem Statement 36

4.2 Cooling of a Hot Surface by Single Droplets 37

4.2.1 Summary of Previous Results

4.2.2 Further Analysis

4.3 Cooling of a Hot Surface by Spray 48

4.3.1 The Model

4.3.2 Sample Calculation

4.4 Nomenclature 67

5. REPORTING ACTIVITIES

5.1 Internal Reports 69

5.2 Presentations 69

5.3 Publications 70

6. SUMMARY AND PERSPECTIVES

6.1 Low Conductivity Solid 71

6.2 Radiation 71

6.3 Spray Cooling 72

7. REFERENCES 73

1. INTRODUCTION

1.1 Background

The long term objective of the study of droplet-solid interactions is to obtain information applicable to the extinguishment of fire through a droplet array (e.g. spray). The solids of concern include porous materials, typical of fire applications.

This report describes the research performed during the period March 1986 - March 1987 under the joint research program conducted by the Center for Fire Research (NBS) and the Mechanical Engineering Department (University of Maryland) addressing the Transient Cooling of a Hot Surface by Droplet Evaporation. This joint research program was initiated in January 1985.

The research described hereafter constitutes the first phase of an extensive research program aimed at developing accurate droplet cooling models of burning solid fuel surfaces. Many studies have been performed to quantify the vaporization process of both single and multi droplet arrays impacting on hot surfaces. For the studies found in the published literature, the full span of the droplet vaporization processes are usually reported. These would include evaporation, nucleate boiling, film boiling and Leidenfrost transition. This present research is more limited in the span of vaporization process studied, being only concerned with the evaporation of single droplets on a hot surface.

The results obtained in the first year of research are twofold. First, a simple mechanism of coupled heat conduction and evaporative mass transfer is

identified as a plausible droplet air boundary condition. This information allows one to model the droplet evaporation in more complex situations where significant, two dimensional temperature gradients are present in both the droplet and the solid. Second, the formulation of a volume of influence in terms of a linear relationship with the evaporation time is the key step to derive a simple model for the cooling effect of a multi-droplet array.

1.2 Overview

On the basis of these two important results, the research effort described in this report encompass several topics.

The experimental results obtained in the first year of study show a strong dependence of the droplet initial configuration (on the solid surface) from the deposition technique. A serious attempt to standardize the droplet deposition procedure was undertaken in the first months of research. The details of the standardized droplet deposition procedure are given in the following sections.

The results for solid of high thermal conductivity, obtained in the first grant period, compared well with similar studies available in the literature. However, the materials of concern in fire research exhibit low thermal conductivity. The information derived from the experiments on aluminum was applied to the study of the thermal behavior of glasslike materials. A first unsuccessful attempt to use regular glass was followed by a complete study of the thermal behavior of Macor. This material exhibits

thermal properties similar to the regular glass but is resistant to the thermal shocks induced by the intense localized droplet cooling.

The data collected in an extensive test matrix were then compiled in a spreadsheet format and plotted in a form suitable for the analysis. The ingredients necessary to develop a complex code for the prediction of the droplet and solid thermal behavior were identified. The governing equations were derived and a number of test cases were solved with the A.D.I. numerical scheme. At that time also the Gauss-Seidel scheme was identified as an alternate numerical method to solve the governing equations.

1.3 Program Development

In this section a brief synopsis of the various research activities is given in the time frame of the reporting period.

Period March 1986 - May 1986 A new deposition device is designed, constructed and successfully tested. A new modular experimental set-up is also designed in order to provide simple interchange of different solid materials in the experimental rig. The A.D.I. numerical scheme is applied to a series of simple test cases.

Period June 1986 - September 1986 The experimental rig is completed in its new configuration. Data for regular glass are collected but, subsequently to the mechanical failure of the glass block, the experiments on glass are terminated. An extensive data collection is performed on Macor. The A.D.I.

numerical scheme is applied to the more complex case of cylindrical coordinates.

Period October 1987 - December 1986 The data collected in the previous period are compiled in spreadsheet format and are plotted in a form suitable for the analysis. Note that during this period Mr. Meng successfully passed the written portion of his comprehensive examination at the University of Maryland.

Period January 1987 - March 1987 The initial development of the code for the simulation of the thermal behavior of both the droplet and the solid is initiated. Simple boundary conditions are applied to test the accuracy of the numerical solution. In parallel with the work of Mr. Meng at the Center for Fire Research, Mr. Wang is hired to perform some preliminary computation on the modelling of the cooling effect of multi-droplet arrays.

2. EXPERIMENTAL MEASUREMENTS

2.1 Deposition Technique

During the course of the aluminum data collection, it was observed that when a liquid droplet is deposited on a solid surface and spreads on it, its final configuration is affected by many factors and varies from one test to another. The volume of the droplet is measured by a micro dispenser which is used to gently deposit the droplet on the solid surface. It was found that the height of the end of the micro dispenser pipette from the solid surface (i.e. the release height of the droplet) is a major factor affecting the final droplet shape. The angle at which the micro dispenser is held with respect to the normal to the surface and the cleanliness of the solid surface are other factors which influence the shape of the droplet.

The evaporation time of a droplet that spreads more on the surface is shorter than the evaporation time of a droplet that spreads less. Therefore, a deposition apparatus is necessary in order to strictly control the droplet release height and the position of the micro dispenser with respect to the surface. Furthermore, an effective technique to clean the surface must also be identified and an identical procedure must be followed for each test.

Figure 1 shows the apparatus designed to deposit the droplet on the solid surface. The micro dispenser is mounted on a support which can be rotated clockwise of 90 degrees in the plane of the drawing. This enables the dispenser to be filled with water. Once the dispenser is in vertical position, it can be locked in place. A motor driven cam actuates the plunger

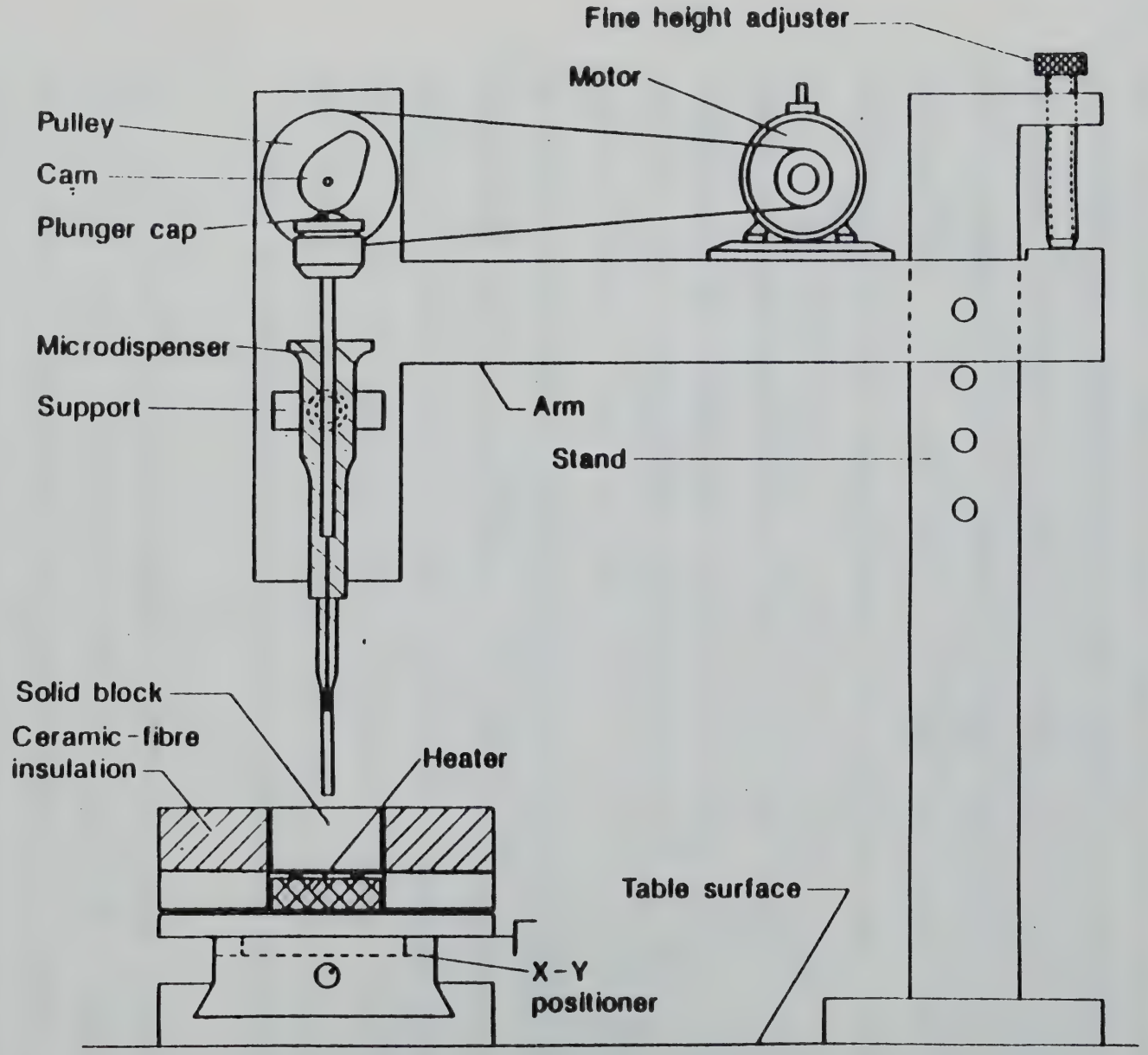

FIGURE 1. Droplet Deposition Apparatus

of the micro dispenser. The cam is designed to execute a down stroke in half revolution followed by an up stroke which takes place in one quarter of a revolution. The last quarter of revolution leaves the plunger at its highest point. The motor speed can be controlled in order to obtain the most desirable deposition cycle.

The height of the micro dispenser pipette with respect to the surface can be closely control by a fine pitch screw at the right end side of the apparatus arm. A substantial stand supports the arm and provides the necessary stability for the apparatus.

The semi-infinite solid on which the droplet is deposited is constituted by a cylindrical block which has a diameter of 10.2 cm and height of 7.6 cm. The block is enclosed in a metal box shown in Fig. 2. The box is divided by an horizontal plate at the lower end of the cylindrical block. The upper portion of the box is filled with ceramic fiber insulation. The lower portion which contains the heater is empty and a number of large holes are drilled in its sides to insure proper ventilation of the heater. The bottom and the sides of the box are made of metal and both the top and intermediate partition are made of insulating, 1 cm thick, slabs. A hole of the same diameter of the cylindrical block is drilled in the top and intermediate plate. The cylindrical block is flush with the upper surface of the box and the heater-solid interface is at the intermediate plate level.

The box contains also the thermocouples which are mounted on the solid

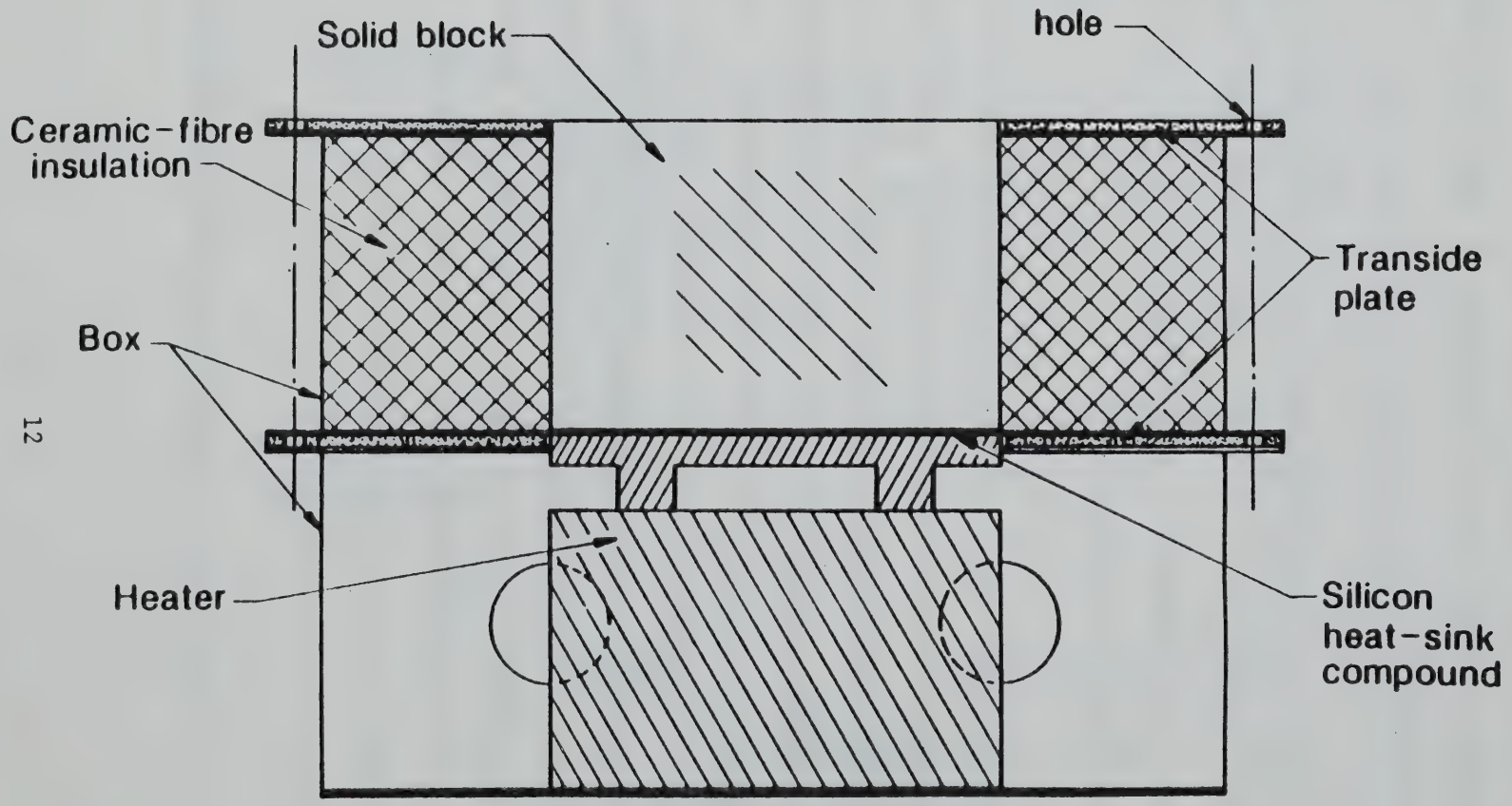

FIGURE 2. Solid Block Modular Enclosure

block. The box is mounted on an x-y positioned that allows the operator to exactly locate the droplet impingement point on the solid surface.

2.2 Experimental Procedures

In the previous year report [1], the properties of the water to be used in the experiments were discussed at length. The water is deionized to eliminate possible salt deposit on the evaporating surface. A complete degassing process is necessary because, otherwise, the droplet shape is altered by the release of the non condensible gasses during the evaporation transient. Furthermore, in the proximity of the nucleation temperature, the non condensible gasses can quickly trigger nucleation, thus completely altering the nature of the droplet vaporization process.

The surface is carefully cleaned first with 98 per cent ethyl alcohol and then with deionized water. Upon complete vaporization of the latter, the actual droplet is deposited. In order to deposit a droplet, the micro dispenser is filled with deionized and degassed water. The cam driven plunger pushes the water out of the micro dispenser pipette. Then the dispenser is rotated away from the surface.

At the deposition time, a stopwatch is activated and a television camera monitors the droplet configuration. The evaporation time is recorded and information on the droplet shape parameter is deduced from the tv recording tape.

The temperature gradient (in the vertical direction) across the cylindrical block, prior to the droplet deposition, provides the necessary information to calculate the heat flux at the solid block upper surface. The convective and radiative components of the flux have not yet been determined due to the lack of information on the emissivity of the Macor surface.

The droplet evaporation time, the shape parameter (e.g. the area of the wetted surface under the droplet), the time dependent history of the droplet shape and the overall heat transfer coefficient at the block upper surface are the data recorded during the various tests.

2.3 Experiments With Glass

The first low conductivity material selected for the experiments was common glass. The upper surface of the glass cylindrical block was polished. The bottom surface was covered with silicon heat sink compound to provide the necessary thermal contact with the heater.

A few droplet were deposited on the block. A small crack due to the intense local thermal stresses was then observed. The crack propagated through the block slowly as more droplets were deposited on the surface.

The clear failure of the common glass due to thermal stresses suggested more strict criteria for the selection of the low conductivity solid materials. Quartz and Macor were then selected.

2.4 Experiments With Macor

The unsuccessful performance of common glass prompted the search for a material that could withstand the thermal shock induced by the localized droplet evaporative cooling. A machinable glass ceramic identified by the tradename: 'Macor' seemed to have the required characteristics. Quartz was also found to satisfy the thermal stress requirements.

The thermal and physical properties of Macor are illustrated in the Fig. 3 through 6. The material was exposed to intense local thermal gradients and it performed according to the expectations. A cylindrical block with polished surfaces was used in the experiments. The dimensions of the block were 10.2 cm in diameter and 7.6 cm in height. The Macor block was mounted in the metal box as previously described for the glass.

2.5 Data Collection

Figure 7 illustrates the location of the various thermocouple on the Macor block. Two sets of three thermocouples are mounted at the top and bottom edges of the block equally spaced along the circumference. The temperature readings are used to infer the top and bottom surface temperatures. The heat flux across the block is then evaluated. In order to obtain information on the convective heat transfer coefficient it is necessary to evaluate the radiative component of the heat flux at the upper surface of the block. Measurements of the Macor emissivity are not available at this time. Figure 8 shows the behavior of the overall heat flux at the surface as a function of the surface temperature. Numerical values for the data points are also given in Table 1.

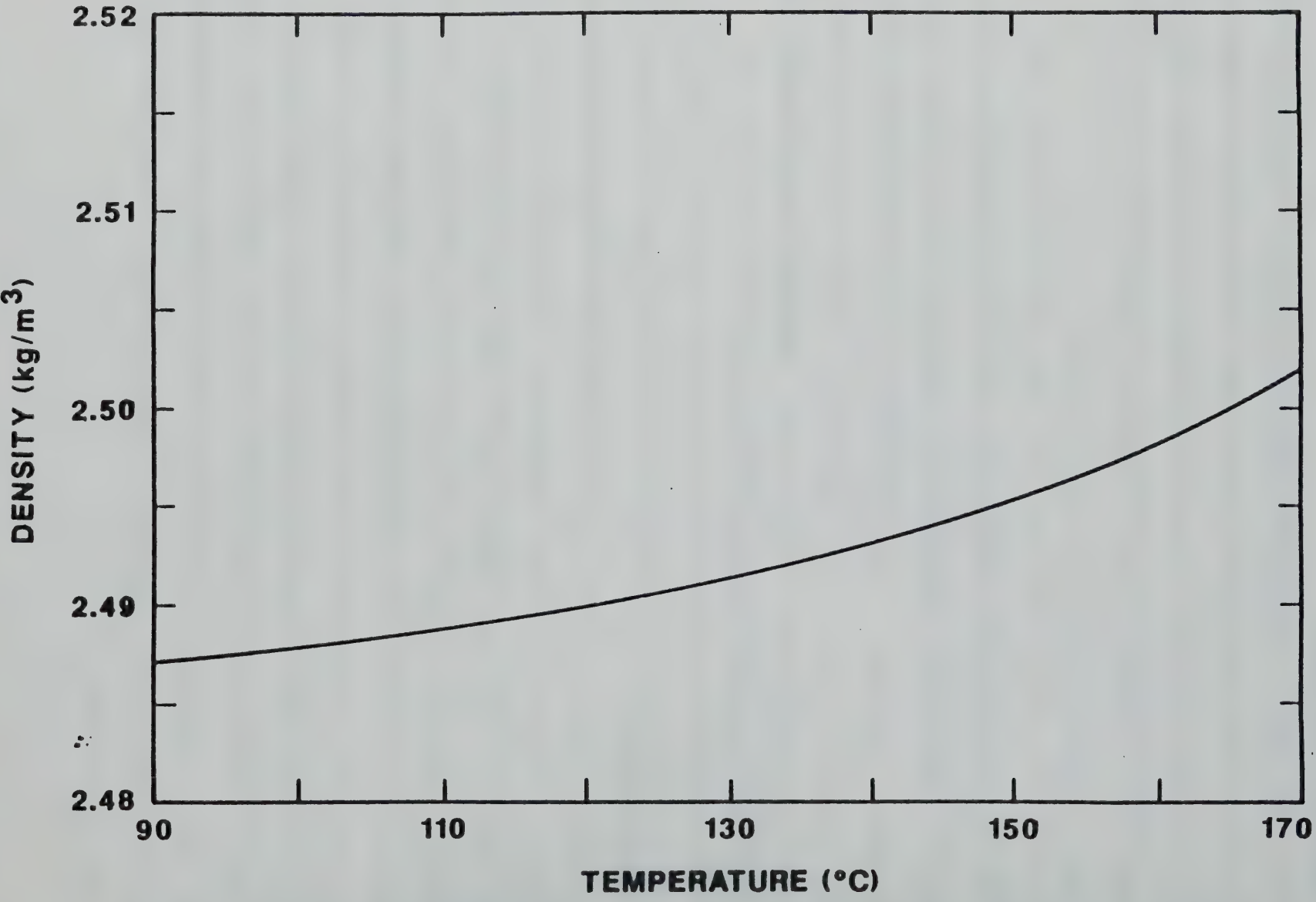

FIGURE 3. Macor Density Versus Temperature

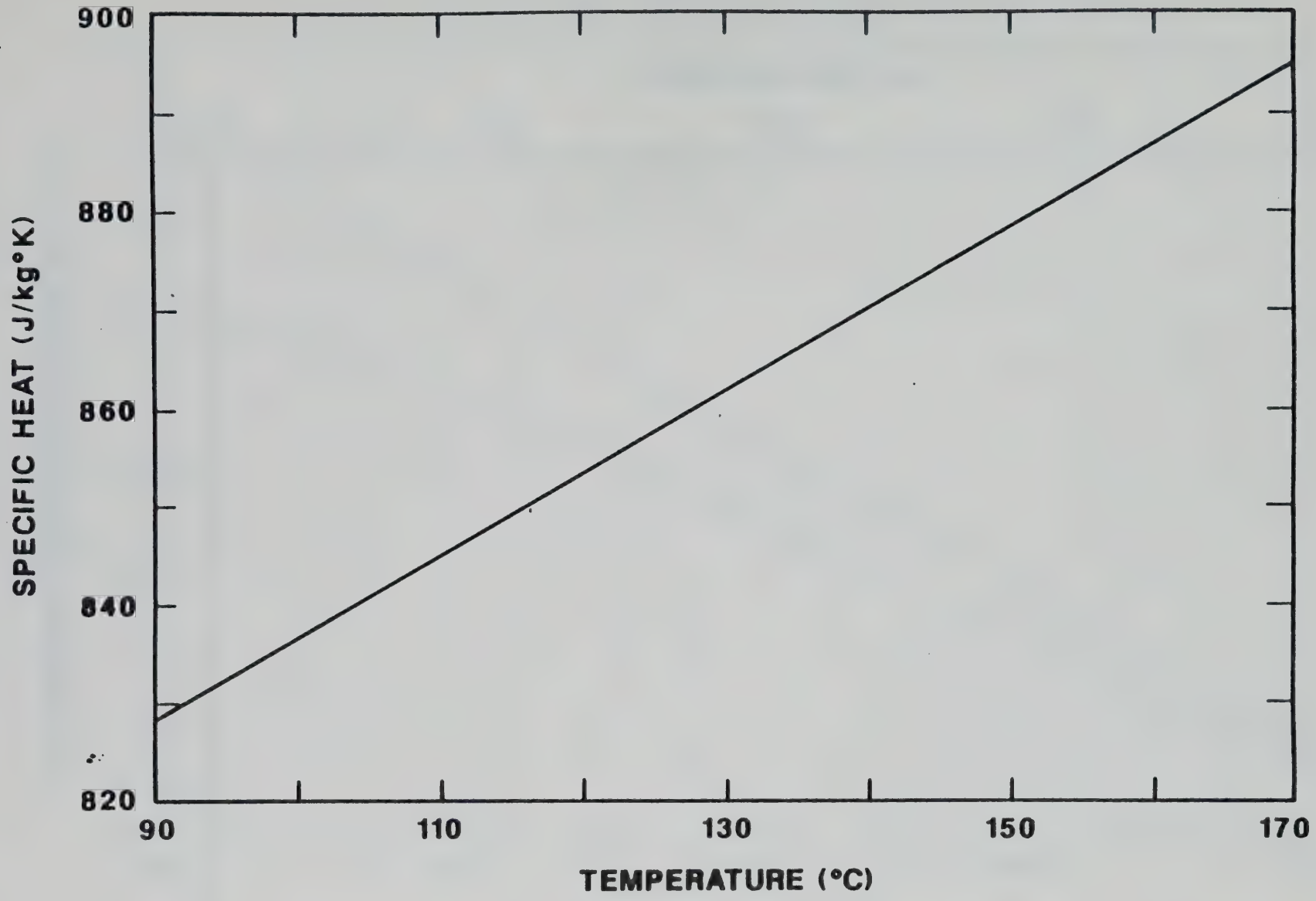

FIGURE 4. Macor Specific Heat Versus Temperature

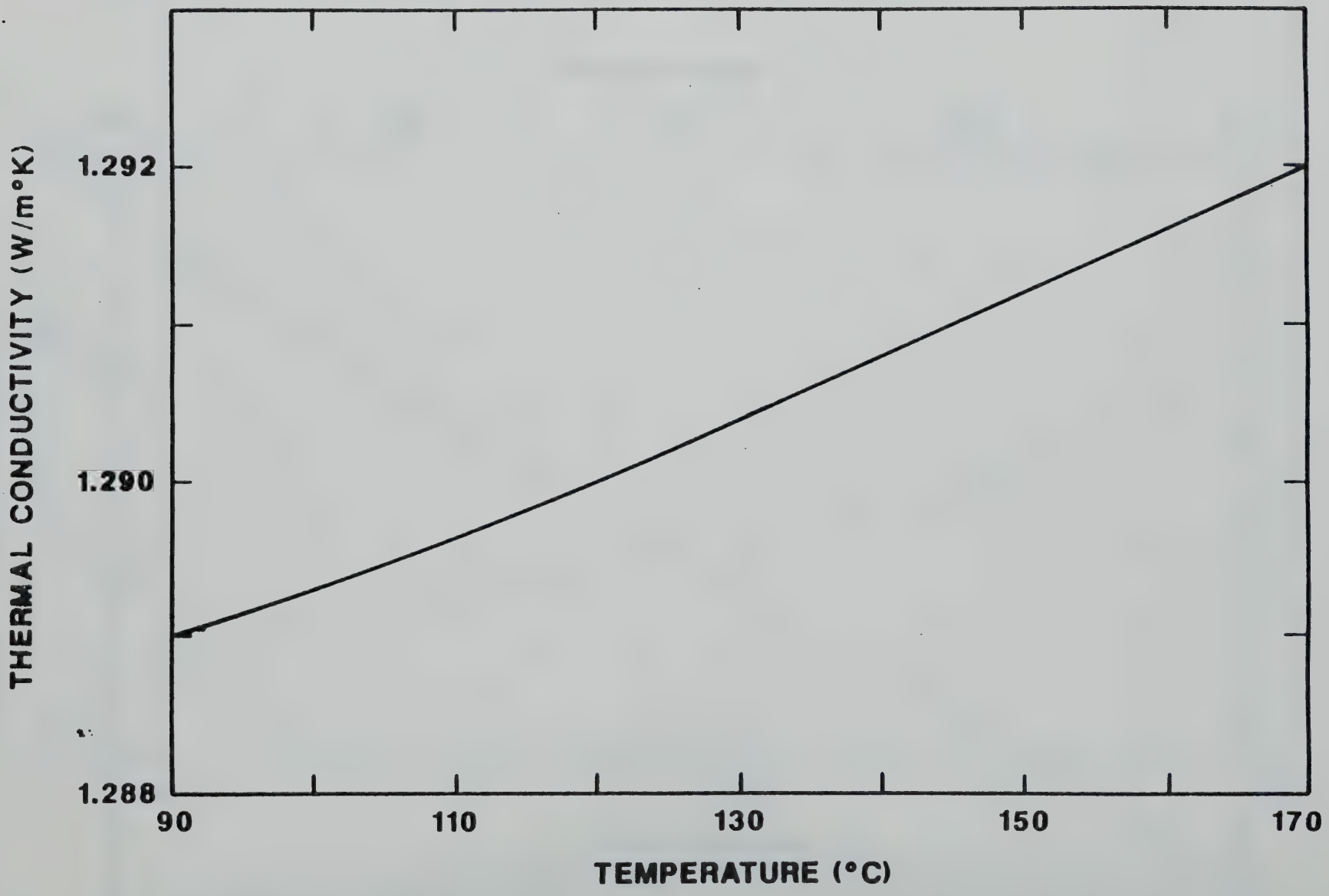

FIGURE 5. Macor Thermal Conductivity Versus Temperature

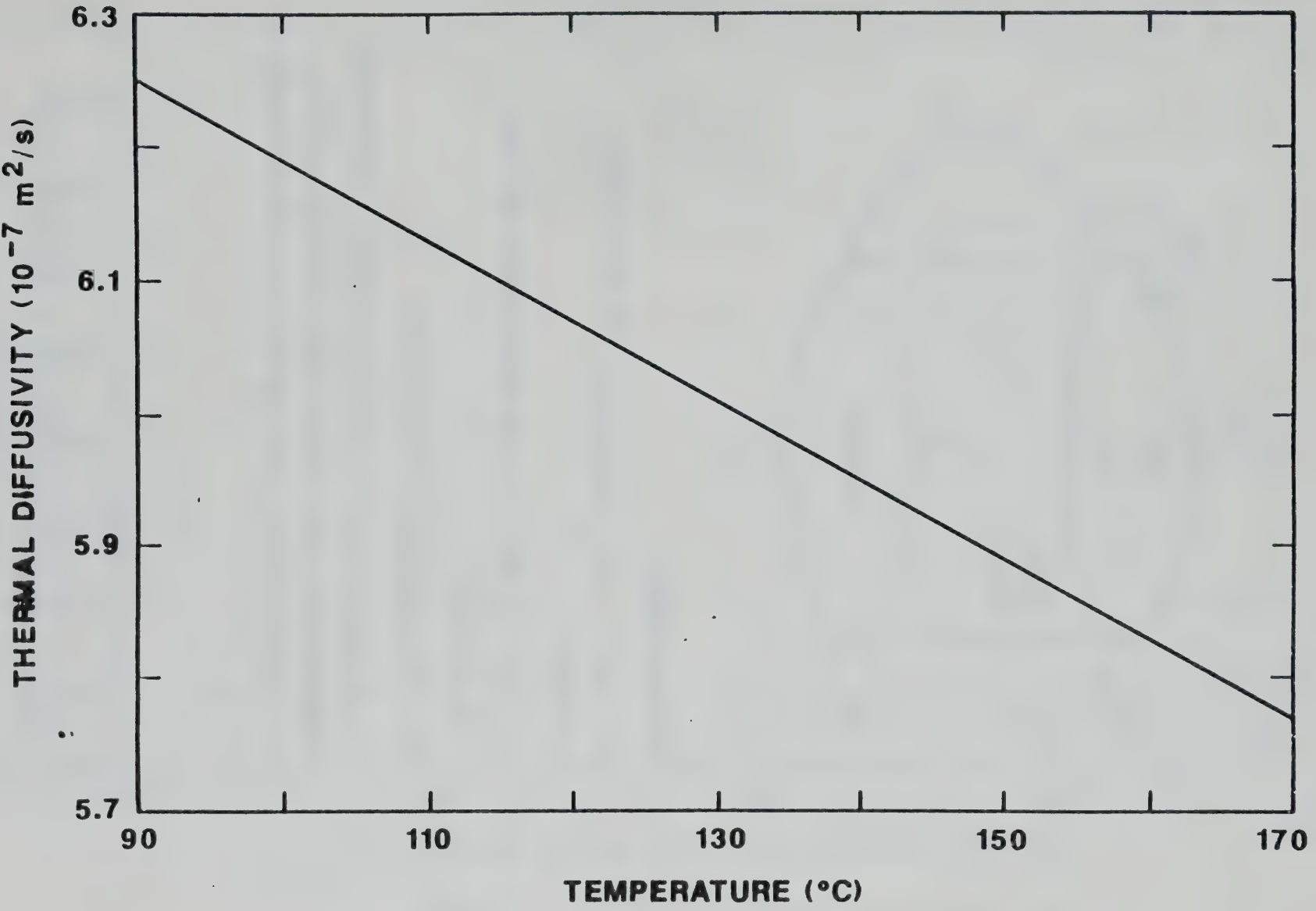

FIGURE 6. Macor Thermal Diffusivity Versus Temperature

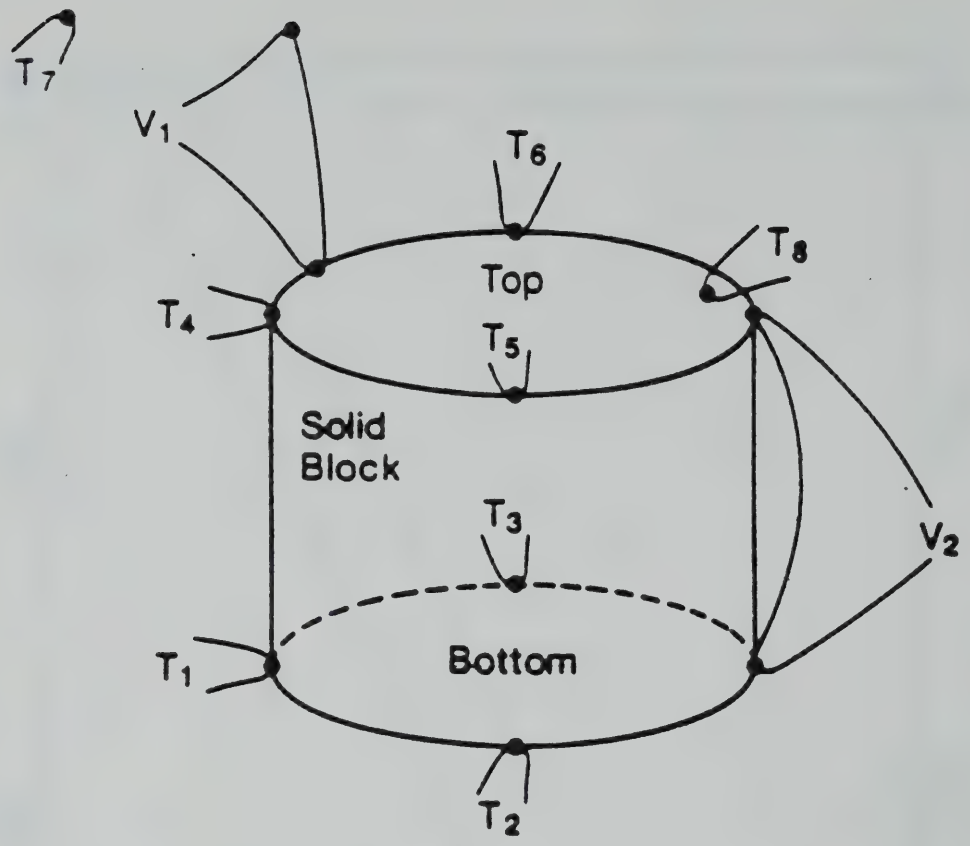

Thermocouples

- T_1, T_2, T_3 are temperature on the bottom surface
- T_4, T_5, T_6 and T_8 are temperature on the top surface
- T_7 is the ambient temperature
- V_1 is proportional to the temperature difference between the top surface and ambient; and V_2 is proportional to the top and bottom surfaces

FIGURE 7. Thermocouple Location on the Macor Block

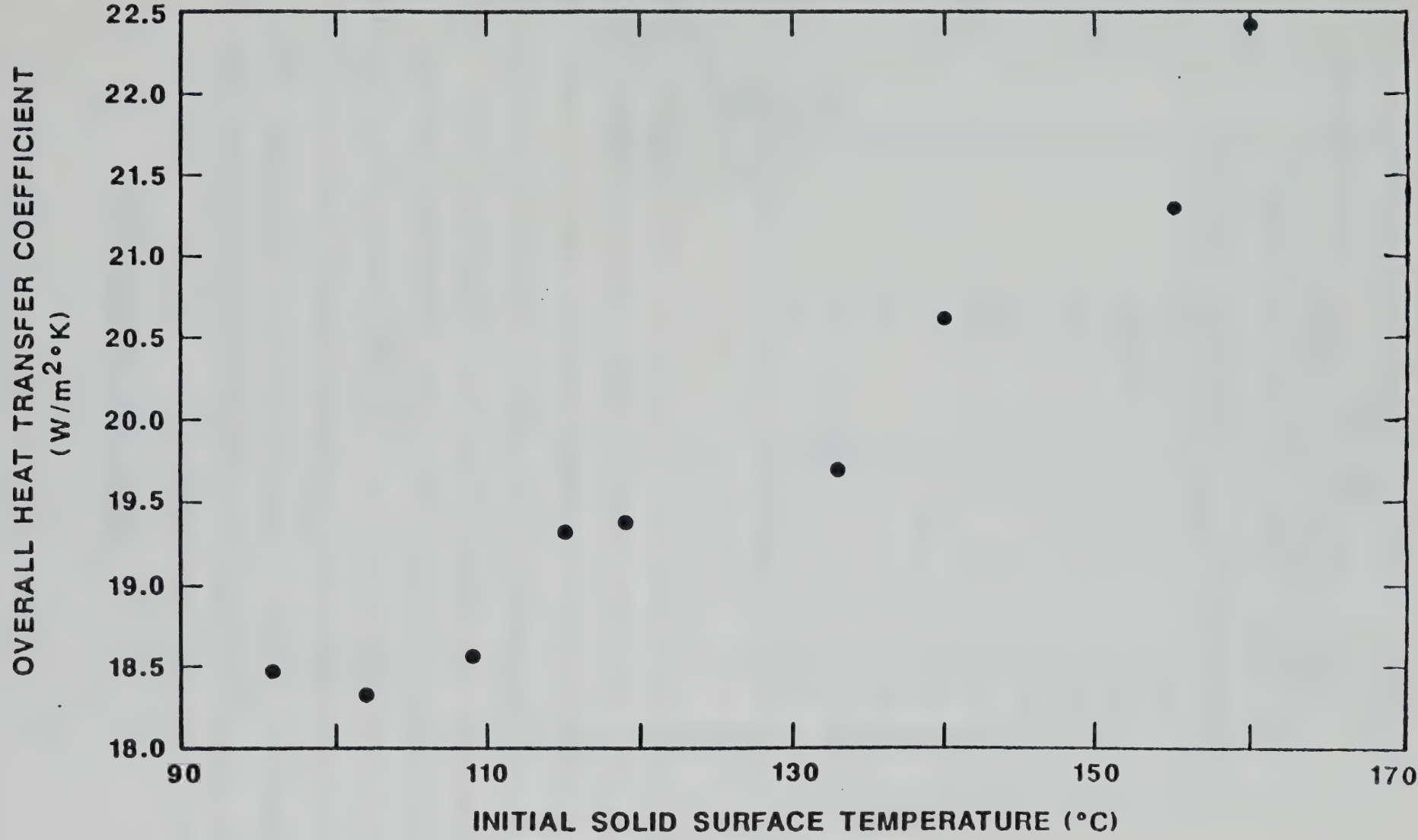

FIGURE 8. Overall Heat Transfer Coefficient at the Upper Surface of the Macor Block Versus the Surface Temperature

TABLE ONE Overall Heat Transfer Coefficient	
Initial Solid Surface Temperature (°C)	Overall Heat Transfer Coefficient (W/m^2 °C)
96	18.5
102	18.3
109	18.6
115	19.3
119	19.4
133	19.7
140	20.6
155	21.3
160	22.4

The radius of the wetted area is measured from the enlarged tv picture of the droplet. An adequate scaling of the tv picture is performed for each test. The measured radius of the wetted area is ratioed to the radius of the spherical droplet of equivalent volume and this information, identified as the shape parameter β_o, is presented in Fig. 9 for various droplet volume versus the initial surface temperature. The data base for the shape parameter includes 300 experimental data points. Each value shown in Fig. 9 and listed in Table 2 is the average of ten consistent experimental measurements. For the purpose of the analysis a constant value of the shape parameter of 1.42 is more than adequate since most of the experimental data are within a plus or minus five per cent band about this value.

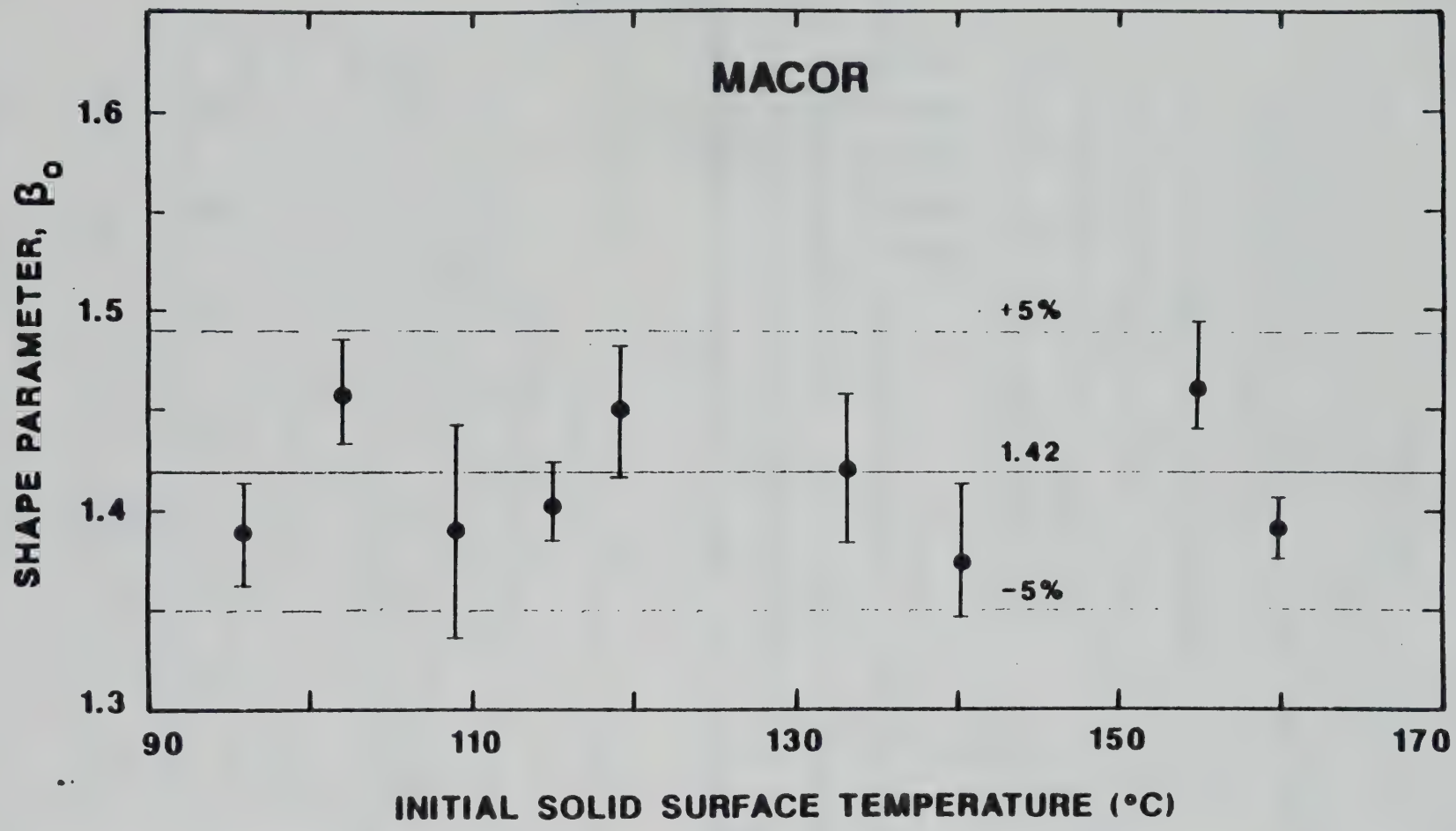

FIGURE 9. Shape Parameter β_o Versus Initial Solid Surface Temperature

TABLE TWO Shape Parameter β_o								
	Initial Solid Surface Temperature (°C)							
Volume (μl)	96	102	109	115	119	133	140	155
10	1.34	1.44	1.42	1.40	1.45	1.43	1.37	1.47
20	1.37	1.45	1.40	1.39	1.48	1.39	1.36	1.46
30	1.40	1.44	1.39	1.42	1.42	1.42	1.35	1.45
40	1.41	1.47	1.42	1.41	1.47	1.46	1.36	1.44
50	1.39	1.46	1.43	1.42	1.48	1.48	1.41	1.49

The evaporation time for various droplet sizes and for various initial surface temperatures are listed in Table 3 and are presented in Fig. 10. The general trend of the evaporation time is in all similar to the trend of the aluminum data (see Fig. 11). Clearly, as expected, the cooling is more

TABLE THREE Evaporation Time (seconds)									
	Initial Solid Surface Temperature (°C)								
Volume (μl)	96	102	109	115	119	133	140	155	160
10	87	74	66	62	53	40	38	28	28
20	117	106	95	84	76	59	51	44	41
30	151	128	117	103	94	73	66	57	54
40	178	155	137	121	111	82	76	66	60
50	210	177	153	137	127	96	86	73	71

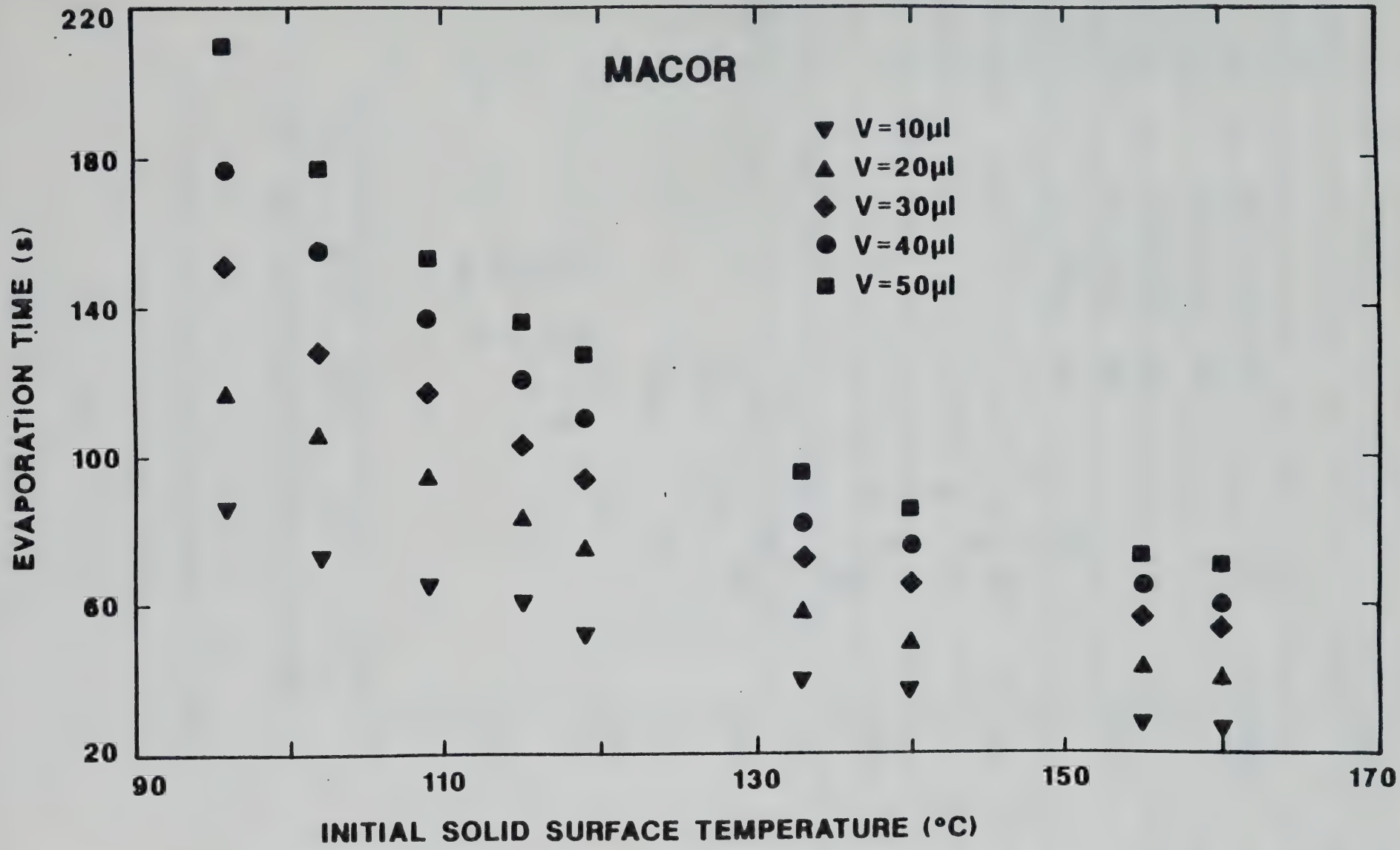

FIGURE 10. Droplet Evaporation Time Versus Initial Solid Surface Temperature (Macor)

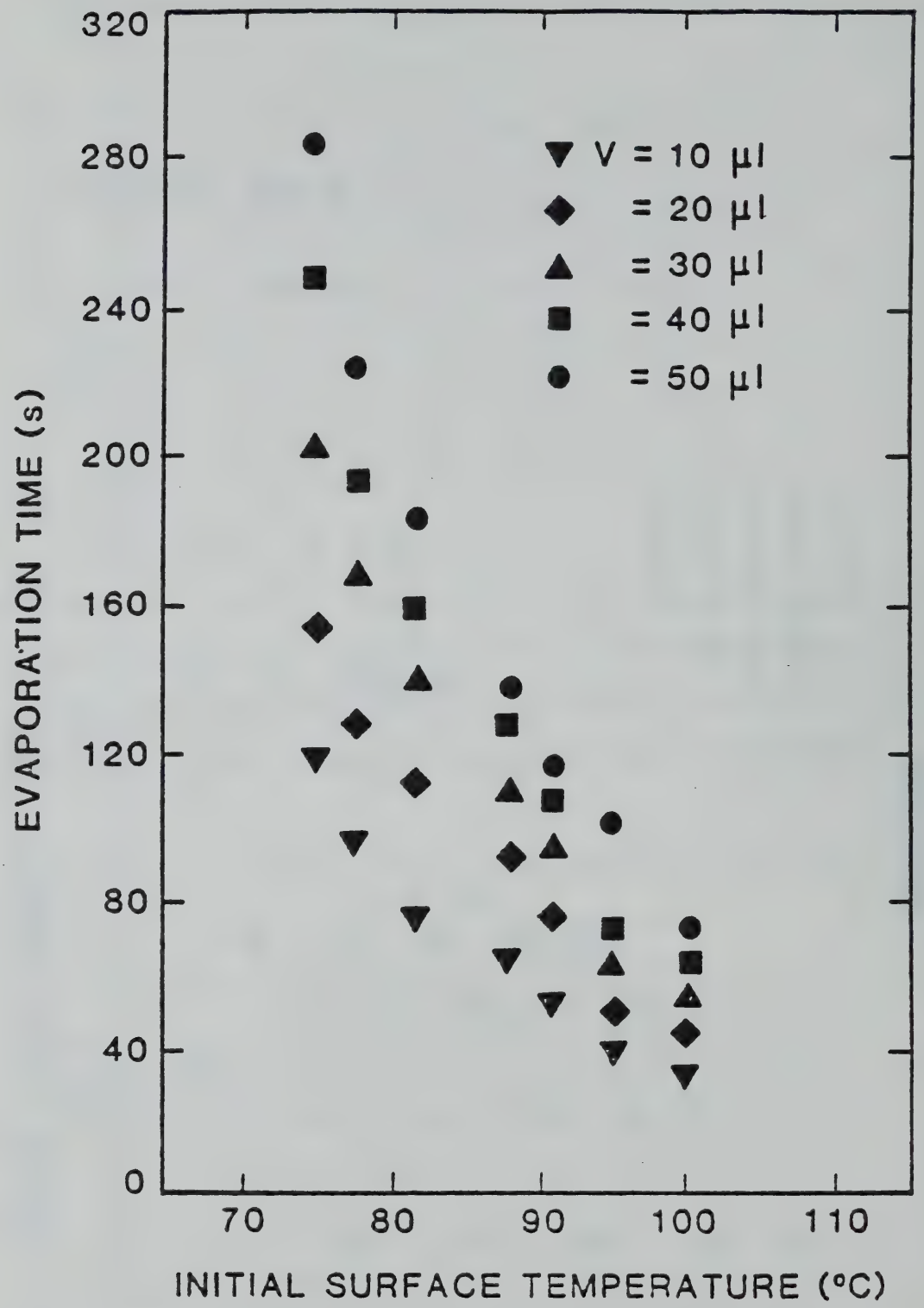

FIGURE 11. Droplet Evaporation Time Versus Initial Solid Surface Temperature (Aluminum)

intense and more localized. This means that the evaporation time for droplet deposited on Macor is longer than the time of evaporation of droplets deposited on aluminum given the same initial surface temperature. The reason for this result is evident if one considers that due to its lower thermal conductivity the Macor exhibits lower temperatures in the droplet proximity than the aluminum. In line with this consideration it is also expected that nucleate boiling is suppressed for initial surface temperatures of the Macor in the order of 160 °C while, for droplets deposited on aluminum, nucleate boiling is observed at few degrees higher than the water saturation temperature. However, if one considers the contact temperature suggested by Seki [2] to be present under the droplet (at least at the initial contact time), it can be shown that, for an initial Macor surface temperature of 160 °C and a liquid water initial temperature of about 25 °C, the contact temperature is very close to the water saturation temperature.

3. THEORETICAL MODEL

3.1 Theoretical Approach

The experimental observation of the droplet evaporative phenomena can provide the necessary information to formulate a predictive model for the droplet evaporation. The validation of such a model is simple because both evaporation time and evaporation rate are easily deduced from the experimental records. More complex to validate and to correctly model is the behavior of the solid under the droplet. The energy balance equation governs the heat transfer in the solid; the boundary conditions to the energy equation are not clearly defined because a number of transport phenomena occurs at the solid-air interface (heat convection, radiation) and at the surface of the droplet (evaporative cooling, heat convection, radiation).

A fundamental difference between high thermal conductivity solids and low thermal conductivity solids must be noted. The cooling is particularly intense at the solid-liquid boundary under the droplet. In a high conductivity solid a large portion of it around the droplet contributes to the heat supply for the droplet evaporation process because heat is transfered with relative ease under small temperature gradients. This is not so for low conductivity material where the limited heat transfer results in a more intense localized cooling in the immediate proximity of the droplet. Large temperature gradients are therefore expected in this case.

The high conductivity of the solid allows one to assume that the temperature at the solid-liquid interface under the droplet is constant and equal to the contact temperature between two semi-infinite bodies as

demonstrated by Seki [2]. For the case of low conductivity materials this assumption is no longer valid and, in order to obtain a boundary condition under the droplet, the coupled solution of the energy equation for the liquid and the solid must be obtained.

In summary, for the case of aluminum, a simple model to predict the droplet evaporation behavior is obtainable without solving the solid energy equation whereas, for the Macor, the solid and the liquid energy equations must be solved simultaneously.

A brief outline of the governing equation and their boundary conditions for the coupled case (Macor) is presented hereafter. Figure 12 represents the coordinate system used in the formulation of equations and boundary conditions.

Solid energy equation

$$\frac{\partial T}{\partial t} = \alpha_S \left(\frac{\partial^2 T}{\partial r^2} + \frac{1}{r}\frac{\partial T}{\partial r} + \frac{\partial^2 T}{\partial z^2}\right) \tag{3.1}$$

Liquid energy equation

$$\frac{\partial T}{\partial t} = \alpha_L \left(\frac{\partial^2 T}{\partial r^2} + \frac{1}{r}\frac{\partial T}{\partial r} + \frac{\partial^2 T}{\partial y^2}\right) \tag{3.2}$$

Boundary conditions

$$@ \quad r = 0 \qquad \frac{\partial T}{\partial r} = 0 \tag{3.3}$$

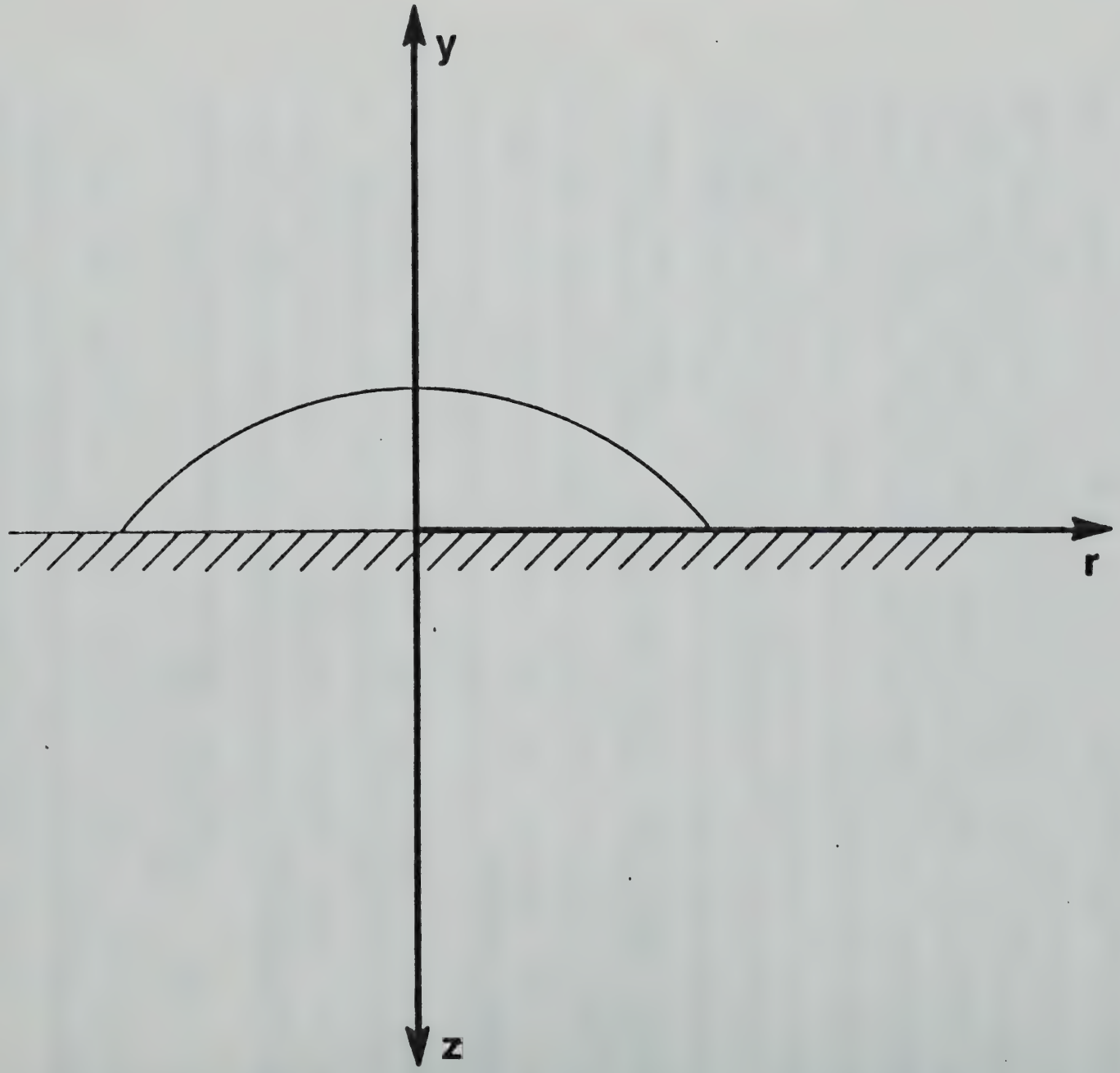

FIGURE 12. Coordinate System

$$@ \quad r \to \infty \qquad \frac{\partial T}{\partial r} = 0 \tag{3.4}$$

$$@ \quad z \to \infty \qquad - k_S \frac{\partial T}{\partial z} = h_A (T_o - T_A) \tag{3.5}$$

$$@ \quad y = z = 0; \quad r \leq R$$

$$k_S \frac{\partial T}{\partial z} = - k_L \frac{\partial T}{\partial y} \tag{3.6}$$

$$(T)_S = (T)_L \tag{3.7}$$

$$@ \quad z = 0; \quad r > R$$

$$- k_S \frac{\partial T}{\partial z} = h_A (T - T_A) + \sigma \epsilon (T^4 - T_A^4) \tag{3.8}$$

$$@ \quad y = f(r) \quad \text{(droplet-air interface)}$$

$$- k_L \frac{\partial T}{\partial z} = h_A (T - T_A) +$$

$$0.624 \left(\frac{D}{\alpha_A}\right)^{2/3} \left(\frac{\Lambda h_A}{c_A}\right) \frac{x - x_A}{1 - x} \tag{3.9}$$

where 0.624 is the air/water molecular weight ratio and f(r) is given by:

$$f(r) = R \left[\frac{(1/a + a)^2}{4} - \left(\frac{r}{R} \right)^2 \right]^{1/2} - \frac{(1/a - a)}{2} \tag{3.10}$$

and

$$a = R\,([\,4/\beta^3 + (1 + 16/\beta^6)^{1/2}]^{1/3} +$$

$$[\,4/\beta^3 - (1 + 16/\beta^6)^{1/2}]^{1/3}) \qquad (3.11)$$

Recall that β is the shape parameter and is defined as the ratio of the radius of the wetted area (which is constant during the evaporation process) over the radius of the equivalent volume spherical droplet. Note that the volume of the droplet is changing as the evaporation takes place.

Initial conditions

(solid)

$$-k_S \frac{\partial T}{\partial z} = h_A (T_o - T_A) \qquad (3.12)$$

(liquid)

$$T = T_A \qquad (3.13)$$

@ $y = z = 0$; $r \leq R$

$$T = \frac{T_o \sqrt{\rho_S c_S k_S} + T_A \sqrt{\rho_L c_L k_L}}{\sqrt{\rho_S c_S k_S} + \sqrt{\rho_L c_L k_L}} \qquad (3.14)$$

3.2 Numerical Methods

In order to solve the previous set of governing equations and boundary conditions two numerical schemes can be used.

The first numerical scheme known as Alternate Directions Iteration (A.D.I.) can be applied separately to the liquid and to the solid. The relevant property of this scheme is the direct solution of the governing equation without iterations. This is due to the simple tridiagonal structure of the matrix to be inverted in order to obtain the solution of the algebraic system of equations obtained by discretizing the original governing equation (partial differential equation in time, radial and axial coordinates). The drawback of this scheme, however, is due to the iterative matching of the solid-liquid boundary conditions. Preliminary trials seem to indicate that in order to obtain a stable solution, one must resort to rather small time increments. Further study of the A.D.I. is necessary prior to obtain meaningful results with this numerical technique.

The second numerical method is iterative but allows one to solve the liquid and the solid at once disregarding the internal boundaries (liquid-solid interface) and considering only the boundaries external to the liquid-solid system. This common numerical scheme is referred to as Gauss-Seidel. The advantage of the direct solution of the two regions is balanced by the less manageable iterative scheme.

Both techniques are considered to solve the energy equation and a comparative evaluation of the results will be performed in the next grant period.

3.4 Nomenclature

a	apex of the droplet (@ r = 0)
c	specific heat at constant pressure
D	air-vapor mass diffusivity
f(r)	equation of the liquid-air interface
h	convective heat transfer coefficient
k	thermal conductivity
R	radius of the wetted area under the droplet
r	radial coordinate tangent to the solid surface
T	temperature
T_o	initial solid surface temperature
t	time
x	vapor molar fraction
x_A	air molar fraction
y	coordinate normal to the solid surface in the liquid
z	coordinate normal to the solid surface in the solid
α	thermal diffusivity
β	shape parameter
ϵ	emissivity of the solid surface
Λ	latent heat of vaporization
ρ	density
σ	Stefan-Boltzmann constant

Subscripts

A	air free stream property
L	liquid property
S	solid property

4. MULTI-DROPLET MODEL

4.1 Problem Statement

The cooling effect induced by the evaporation of a single droplet on an aluminum surface has been measured and evaluated by diMarzo and Trehan [1]. Their study is the basis for the development of a multi-droplet model.

The present study is aimed at developing a multi-droplet model on the basis of the single droplet information. Two questions must be addressed by the multi-droplet model. They are:

1. How much water is sufficient for cooling the hot surface?

2. What is the most efficient way of spraying water on the hot surface?

Since the multi-droplet model incorporates experimental results of the single droplet experiment, the applicability of this model is confined within these experimental conditions. However, the concept and methodology employed in the model is not subjected to these restrictions. If a broader range of experimental data is available, the concept and methodology proposed in this study can be used to develop a similar multi-droplet model with wide applicability.

In the following sections, a brief summary of the single droplet experiment and further analysis of the data are presented. Subsequently, a multi-droplet model is proposed and sample calculations are made.

4.2 Cooling of a Hot Surface by Single Droplets

The cooling effect induced by the evaporation of a single droplet on a hot semi-infinite aluminum block was investigated by diMarzo and Trehan [1]. In this section, a brief summary of their results is presented. Also presented is a further analysis of their experimental data. This analysis leads directly to the development of a multi-droplet evaporation model.

4.2.1 Summary of the Previous Results The study of diMarzo and Trehan [1] includes both the experimental and theoretical aspects. The experiments and the computer code simulation provide information on the cooling effect induced by an evaporating water droplet in a hot aluminum block simulating a semi-infinite body. The droplet is 'gently' deposited on the aluminum surface by a graduated hypodermic siring. The initial surface temperature ranges from 75 °C to 100 °C; implying a full suppression of nucleate boiling. Thus, only evaporation takes place. The diameter of the spherical droplet prior to deposition on the surface varies from 0.8 mm to 4.5 mm. The detail of the experimental conditions can be found in Ref. [1]. In general, the following two main conclusions are the result of the study:

1. The parameter β_o, proposed by Bonacina [4], is defined as the ratio of the droplet diameter after deposition (d) to that before deposition (D). Figure 13 illustrates its definition. Since the parameter β_o characterizes the geometrical configuration of the droplet on the surface, it is an important parameter determining the droplet evaporating time and its cooling effect. It was found that if a droplet is gently deposited on an aluminum surface, the value of the parameter

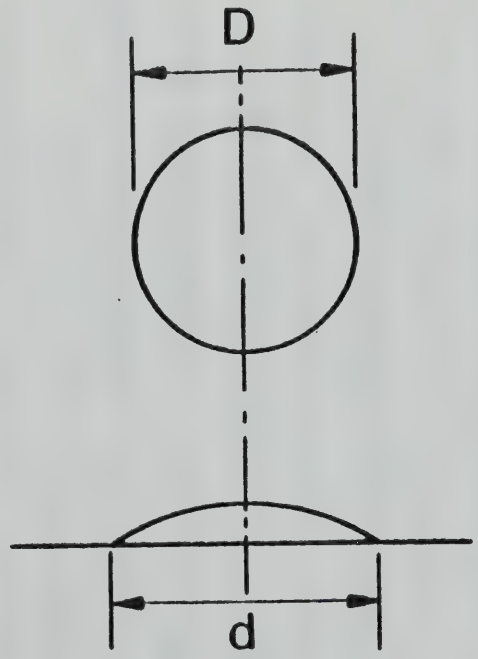

Parameter $\beta = d/D$

	Typical β value
• Gently deposited droplet	~ 1.3
• Impinging spray	~ 4.3

FIGURE 13. Shape Parameter Definition

β_o can be represented by a linear regression equation with an error bar of +/- 5% (Fig. 14). This equation can be written as

$$\beta_o = d/D = 0.6 + 0.009 * T_s \qquad (4.1)$$

where T_s is the initial surface temperature (°C)

2. The evaporation time was found to be an exponential function of the initial surface temperature and a power function of the droplet volume. A logarithmic regression analysis generates the following equation:

$$\tau = 876. * V^{(0.7)} \, e^{(-0.07 \, T_s)} \qquad (4.2)$$

where τ is the droplet evaporation time (sec) and V is the droplet volume (μl). This equation yields values which are in the range of +/- 20% of the experimental values.

On the basis of the experimental data, a computer code was set up to calculate the thermal behavior of the semi-infinite solid in the neighborhood of an evaporating droplet.

The concept of the volume of influence was proposed to quantify the cooling effect induced by an evaporating droplet. The volume of influence is defined as the volume of the region of the solid where the temperature drop

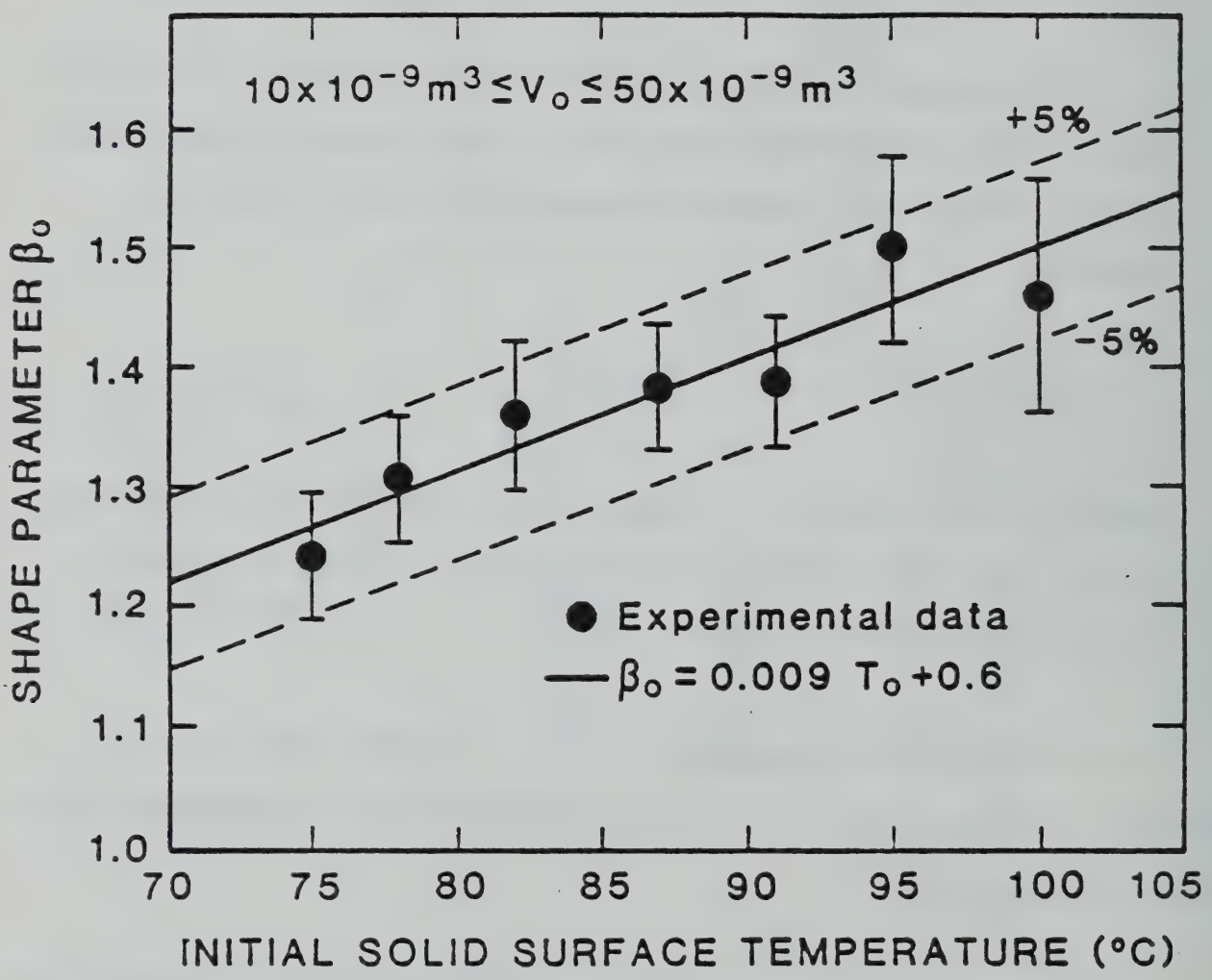

FIGURE 14. Shape Parameter Versus Initial Solid Surface Temperature

due to the droplet evaporation is at least 10% of the maximum possible temperature drop. This parameter is a function of several variables:

1. The evaporation time

2. The volume of the droplet

3. The initial surface temperature

4. The convective heat transfer coefficient

It was found that a linear relationship exists between the maximum volume of influence (V_i/V) and the evaporation time (τ). The relationship is represented by the following equation (See also Fig. 15):

$$V_i/V = 3 + 0.012\ \tau \qquad (4.3)$$

This linear relationship is fundamental for the developement of the multi-droplet model.

4.2.2 Further Analysis On the basis of the volume of influence concept, two additional concepts can be defined in a similar way: the area and the radius of influence. The area and radius of influence are, respectively, the area and radius of the hot solid surface where the temperature drop due to a droplet evaporation is at least 10% of the maximum possible temperature drop.

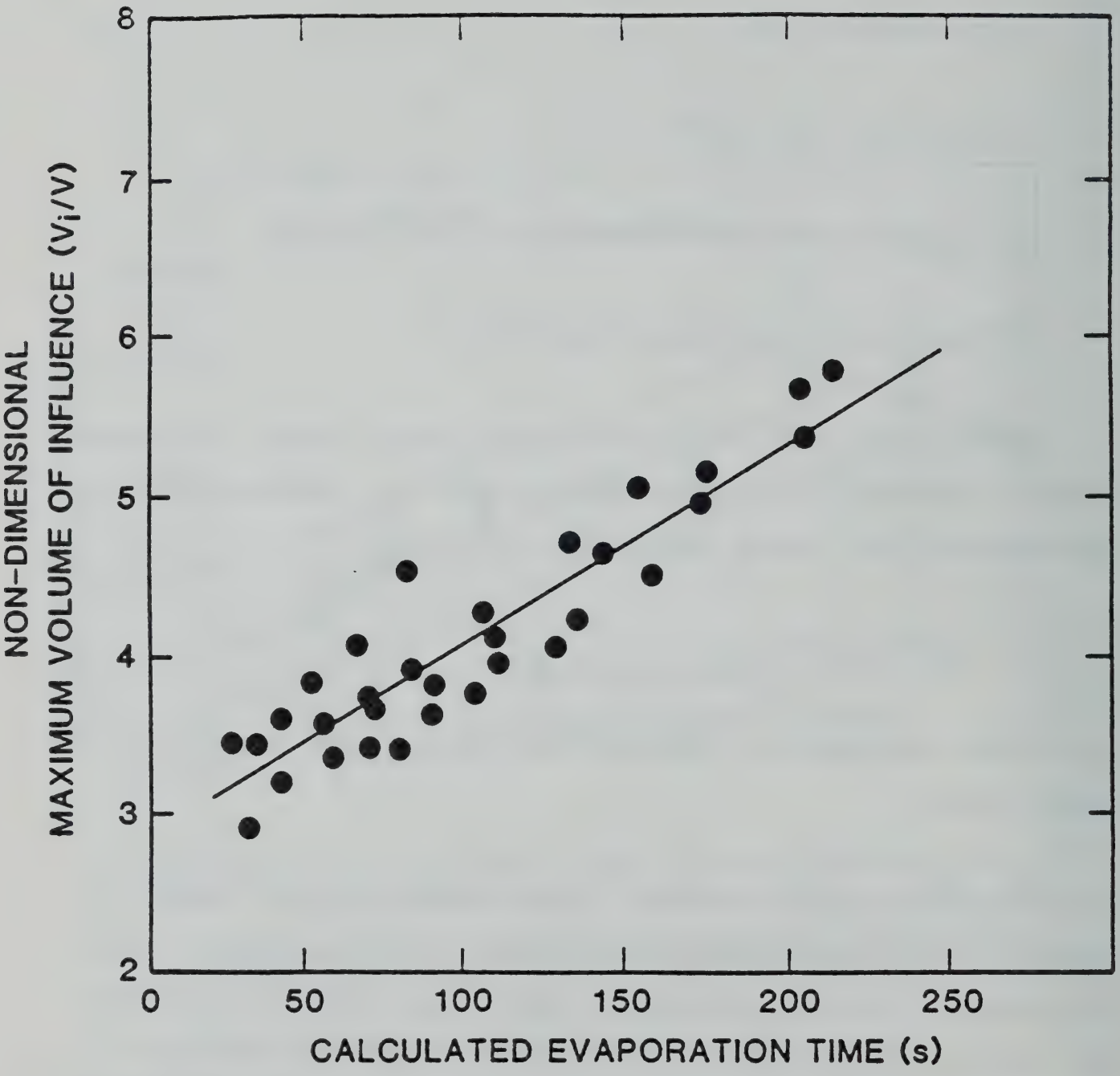

FIGURE 15. Non-Dimensional Volume of Influence Versus Evaporation Time

An effort is made to correlate the maximum area and radius of influence with the droplet evaporation time.

Figure 16 shows the maximum area of influence (A_i) as a function of the evaporation time for various droplet volumes and initial surface temperatures. It is found that no clear relationship exists between these two parameters. If the maximum area of influence is non-dimensionalized by the cross sectional area of droplet before deposition (A_D), this non-dimensional parameter (A_i/A_D) does not correlate with the evaporation time either (Fig. 17). However, if the maximum area of influence is non-dimensionalized by the area of droplet after depositing (A_d), the non-dimensional parameter (A_i/A_d) correlates linearly with the evaporation time (Fig. 18). The linear regression of the data points can be expressed as:

$$A_i/A_d = 2.161 + 0.042\ \tau \qquad (4.4)$$

Similarly, the non-dimensional maximum radius of influence (r_i/r_d), also correlates linearly with the evaporation time (Fig. 19); that is:

$$r_i/r_d = 1.73 + 0.0075\ \tau \qquad (4.5)$$

These two linear functions are important, since they are used directly to develop the multi-droplet model.

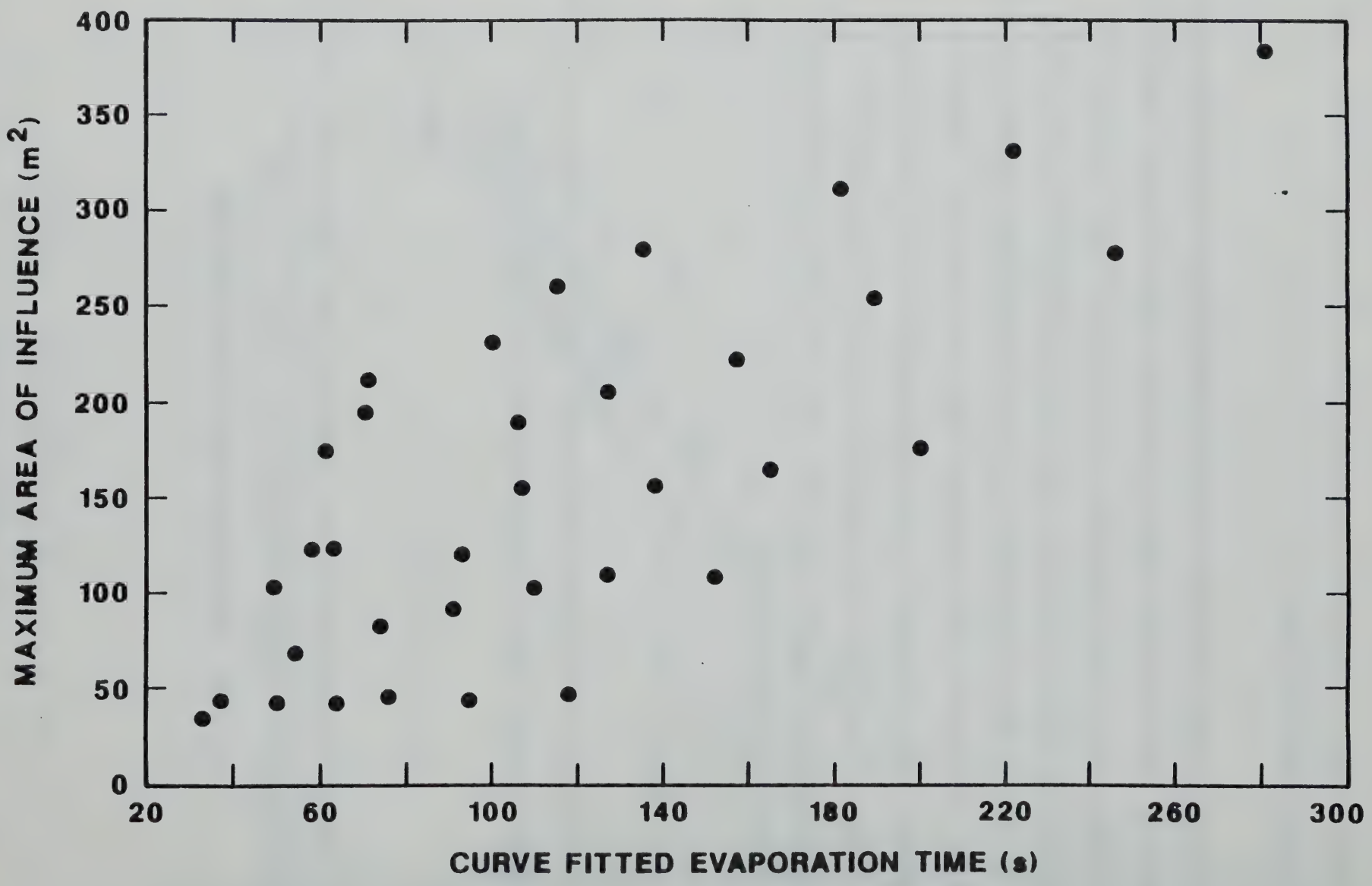

FIGURE 16. Maximum Area of Influence Versus Evaporation Time

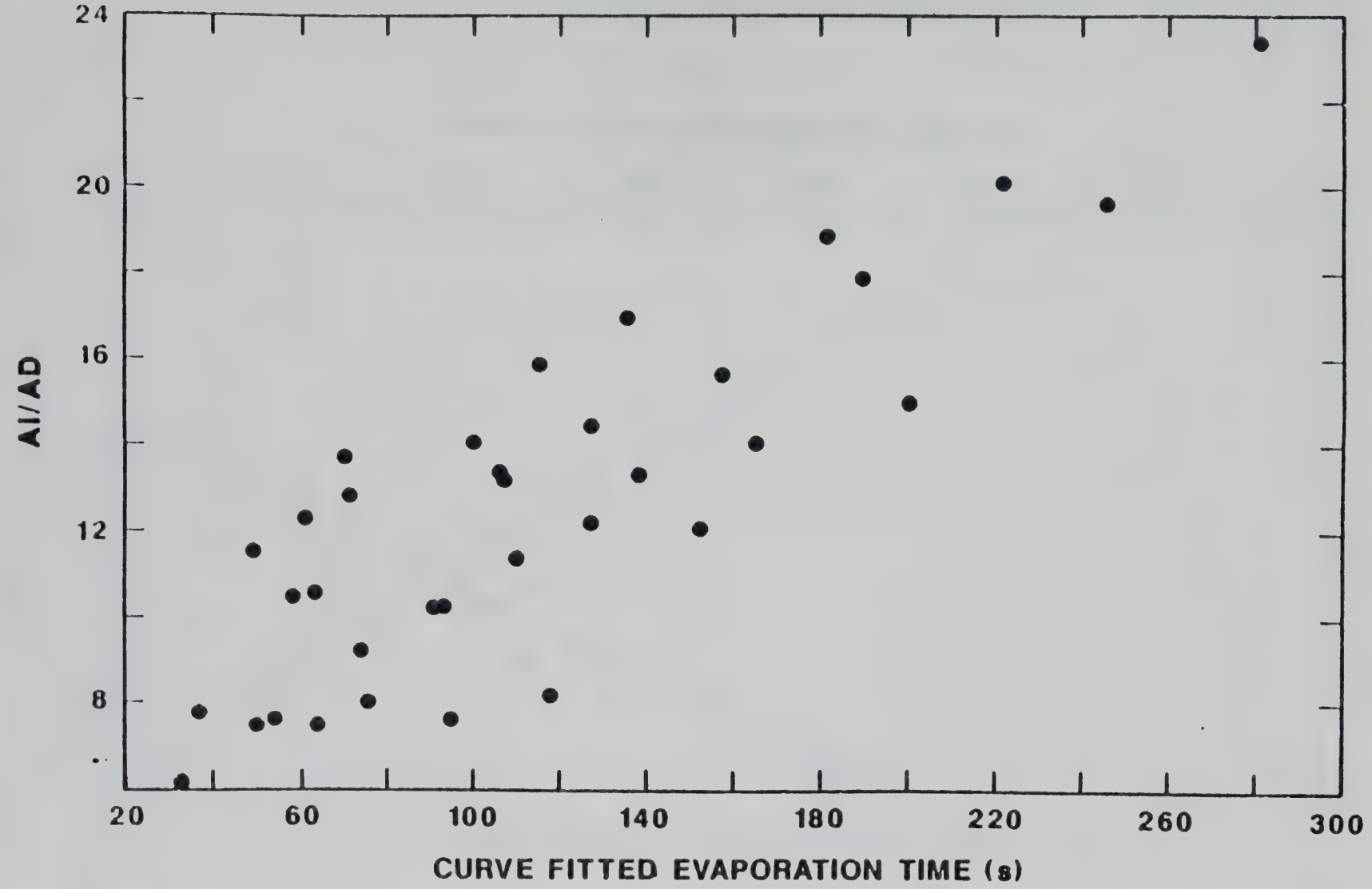

FIGURE 17. Non-Dimensional Area of Influence (w.r.t. spherical droplet cross-sectional area) Versus Evaporation Time

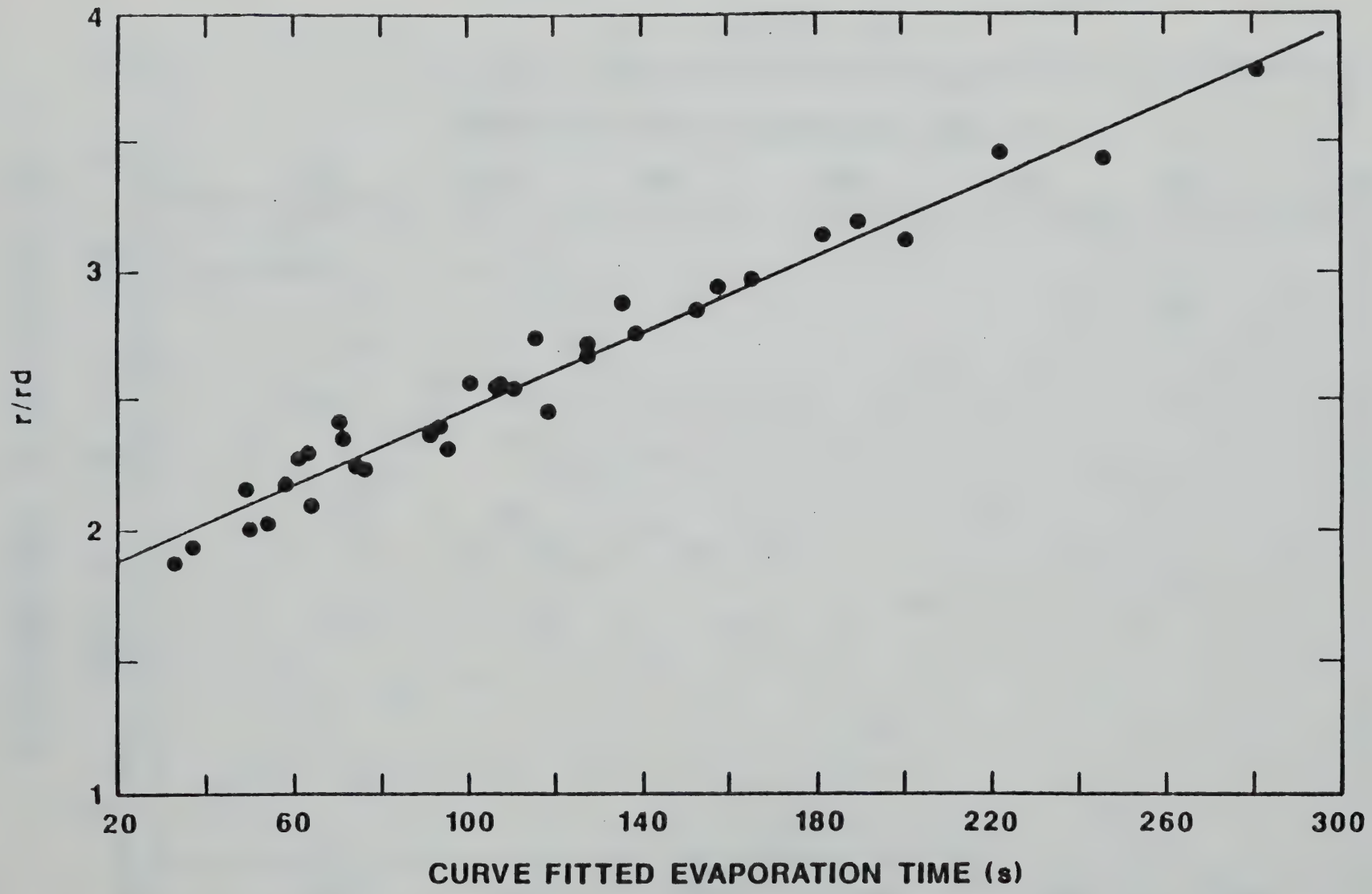

FIGURE 19. Non-Dimensional Radius of Influence (w.r.t. radius of the wetted region) Versus Evaporation Time

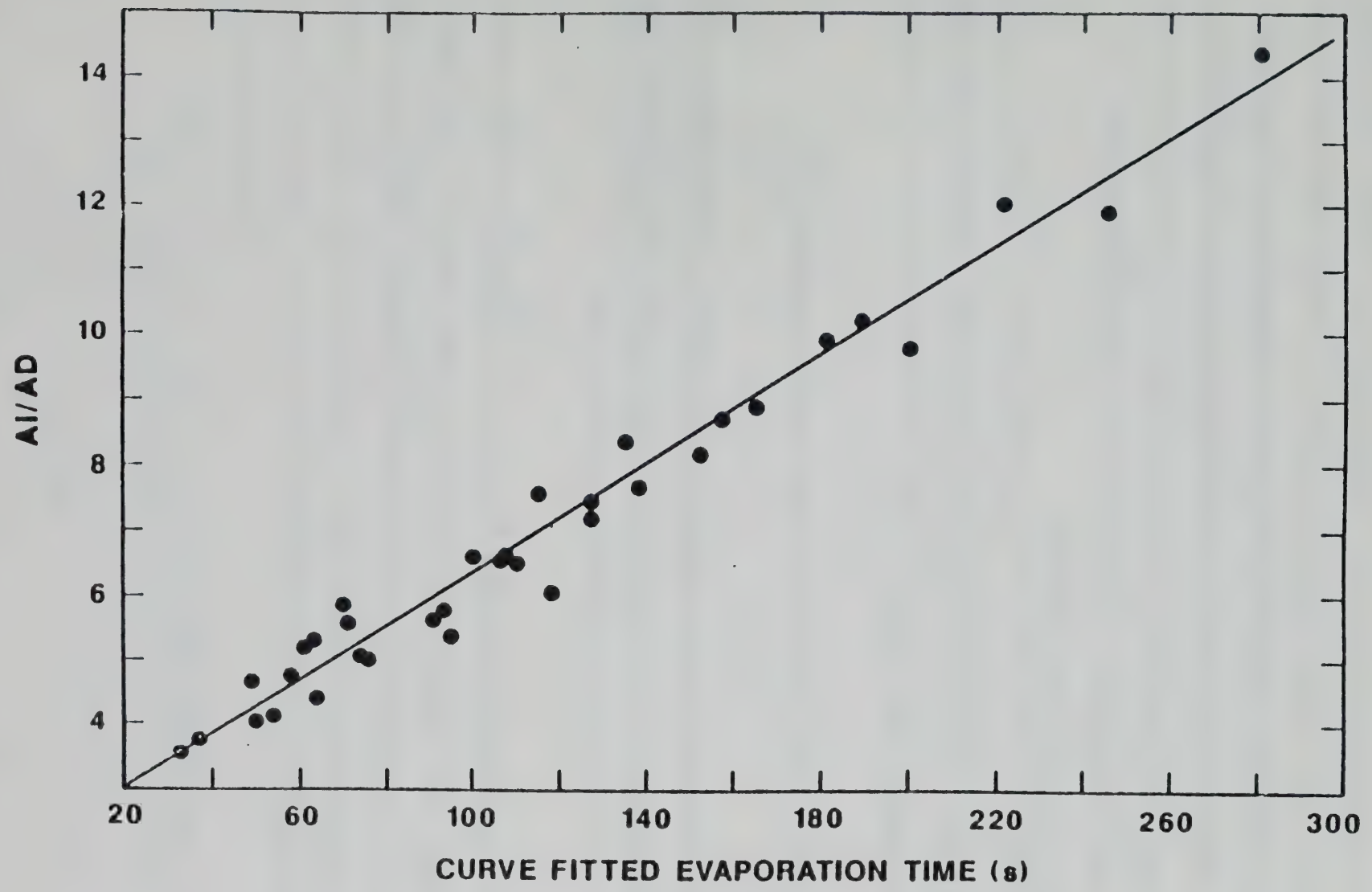

FIGURE 18. Non-Dimensional Area of Influence (w.r.t. area of the wetted region) Versus Evaporation Time

4.3 Cooling of A Hot Surface by A Spray

On the basis of the results of a single evaporating droplet, the cooling effect induced by a spray can be evaluated by taking into account the distribution of droplet sizes. In this study, a general model, which can be used for different types of droplet distribution functions and thus different types of sprays, is developed. By using this model, some sample calculations are also made to predict the minimum droplet mass per unit surface area necessary for the hot surface cooling.

4.3.1 The Model In order to develop the general multi-droplet model, the following assumptions are needed:

1. No coalescence of droplets takes place on the surface

2. A suitable frequency function can describe the distribution of droplet sizes in the spray (the Rosin-Rammler [3,4], the Log-Probability [3] and the Nukiyama-Tanasawa [3,5] distributions).

The droplet size distribution function can be written in several forms. In this study, the 'volume distribution' form is used; that is, dv/dD, where v is the volume fraction and D is the diameter of a droplet. Thus, the mass of droplets having diameter between D and D + ΔD that reach the surface between the time instant t and t + Δt is given by:

$$\Delta(\Delta m) = (W_s \Delta t) \left(\frac{dv}{dD}\right) \Delta D \qquad (4.6)$$

where W_s is the mass flow rate of the droplet deposited on the hot solid surface.

Therefore, the maximum area of influence produced by $\Delta(\Delta m)$, Eq. (4.6) can be expressed by the following equation:

$$\Delta(\Delta A_i) = \frac{\Delta(\Delta m)}{m_d} \Delta A_i \tag{4.7}$$

where m_d is the mass of a droplet and ΔA_i is the maximum area of influence induced by a droplet. Equation (4.7) can be non-dimensionalized with respect to the total hot solid surface area A; that is:

$$\frac{\Delta(\Delta A_i)}{A} = \frac{\Delta(\Delta m)}{A} \frac{\Delta A_i}{m_d} \tag{4.8}$$

For a single droplet, $\Delta A_i/m_d$ can be expressed in terms of the droplet diameter D, and the initial surface temperature T_s. It can be shown that:

$$\frac{\Delta A_i}{m_d} = \frac{\Delta A_i}{A_d} \frac{A_d}{m_d}$$

$$= \frac{\Delta A_i}{A_d} \left(\frac{\pi}{4} \beta^2 D^2\right)/\left(\frac{\pi}{6} D^3 \rho_d\right) \tag{4.9}$$

By substituting Eqs. (4.1) and (4.4) into the above equation, one can obtain the following result:

$$\frac{\Delta A_i}{m_d} = \frac{(2.161 + 0.042\,\tau)\,(1.5)\,(0.6 + 0.01\,T_s)^2}{\rho_d\, D} \tag{4.10}$$

Since τ is given by Eq. (4.2), the above equation can be recasted as:

$$\frac{\Delta A_i}{m_d} = C(T_s) \left[\frac{0.092}{D} + D\, e^{(-0.05\, T_s)}\right] \tag{4.11}$$

where $C(T_s)$ is a function T_s; i.e.,

$$C(T_s) = 3.5 * 10^{-3} (60 + T_s)^2/\rho_d \tag{4.12}$$

By combining Eqs. (4.6),(4.8) and (4.11), the following equation is obtained:

$$\frac{\Delta A_i}{A} = (W_s\, \Delta t)\, C(T_s) \left[\frac{0.092}{D} + D\, e^{(-0.05\, T_s)}\right] \frac{dv}{dD}\, \Delta D \tag{4.13}$$

where W_s is the droplet mass flow rate in a spray.

The total fraction of maximum area of influence produced by a spray of droplets having diameter ranging from D_o to D_m that reach the surface between the time t and t + Δt can be found by an integration of Eq. (4.13) over the droplet diameter range D_o to D_m:

$$\frac{A_i}{A} = (W_s\, \Delta t)\, C(T_s) \int_{D_o}^{D_m} \left[\frac{0.092}{D} + D\, e^{(-0.05\, T_s)}\right] \frac{dv}{dD}\, dD$$

$$= (W_s\, \Delta t)\, C(T_s) \left[0.092 \int_{D_o}^{D_m} \frac{dv}{dD} \frac{dD}{D} \right.$$

$$\left. + e^{(-0.05\, T_s)} \int_{D_o}^{D_m} \frac{dv}{dD}\, D\, dD \right] \tag{4.14}$$

The two integration terms in Eq. (4.14) designate two different orders of mean diameters of a spray. In Ref. [3], the mean diameter $\bar{D}_{qp}$ of order p + q is defined by:

$$\bar{D}_{qp}^{q-p} = \left[\int_{D_o}^{D_m} D^q \frac{dn}{dD}\, dD\right] / \left[\int_{D_o}^{D_m} D^p \frac{dn}{dD}\, dD\right] \qquad (4.15)$$

where Δn is the number fraction of droplets having diameter between D and D + ΔD. The mean diameters $\bar{D}_{qp}$ can also be given in terms of Δv; i.e., the volume fraction of droplets having diameters between D and D + ΔD.

$$\bar{D}_{qp}^{(q-p)} = \left[\int_{D_o}^{D_m} D^{(q-3)} \frac{dv}{dD}\, dD\right] / \left[\int_{D_o}^{D_m} D^{(p-3)} \frac{dv}{dD}\, dD\right] \qquad (4.16)$$

Note that in many mass transfer and flow process [3], it is desirable to work only with mean diameters instead of the complete droplet distribution. Table 4 shows some of the mean diameters and some of their respective fields of application. These mean diameters can be readily calculated from the droplet size distribution equation.

Consequently, according to the definition of the mean diameter, Eq. (4.12), the two integration terms in the Eq. (4.14) can be interpreted as $(\bar{D}_{32})^{-1}$ and $\bar{D}_{43}$ respectively; that is,

$$\bar{D}_{32} = \left[\int_{D_o}^{D_m} D^3 \frac{dn}{dD}\, dD\right] / \left[\int_{D_o}^{D_m} D^2 \frac{dn}{dD}\, dD\right]$$

$$= \left[\int_{D_o}^{D_m} \frac{dv}{dD}\, dD\right] / \left[\int_{D_o}^{D_m} \frac{dv}{dD} \frac{dD}{D}\right] = 1 / \left[\int_{D_o}^{D_m} \frac{dv}{dD} \frac{dD}{D}\right] \qquad (4.17)$$

TABLE FOUR

Mean Diameters [3] (Cfr. Eq. 12)

p	q	p+q	Mean Diameter	Application
0	1	1	Linear	Evaporation
0	2	2	Surface	Absorption
0	3	3	Volume	Hydrology
1	2	3	Surface Dia.	Adsorption
1	3	4	Volume Dia.	Diffusion
2	3	5	Sauter Dia.	Mass Transfer
3	4	7	DeBrouckere Dia.	Combustion

and,

$$\bar{D}_{43} = \left[\int_{D_o}^{D_m} D^4 \frac{dn}{dD}\, dD\right] / \left[\int_{D_o}^{D_m} D^3 \frac{dn}{dD}\, dD\right]$$

$$= \left[\int_{D_o}^{D_m} \frac{dv}{dD} D\, dD\right] / \left[\int_{D_o}^{D_m} \frac{dv}{dD}\, dD\right]$$

$$= \int_{D_o}^{D_m} \frac{dv}{dD} D\, dD \qquad (4.18)$$

Therefore, one can write

$$\frac{A_i}{A} = (W_s\, \Delta t)\, C(T_s) \left[\frac{0.092}{\bar{D}_{32}} + \bar{D}_{43}\, e^{(-0.05\, T_s)}\right] \qquad . (4.19)$$

where $\bar{D}_{32}$ is commonly called the sauter mean diameter and $\bar{D}_{43}$ is referred to as the DeBrouckere diameter.

Note that these two mean diameters are related to the surface and volume of the droplets in a spray. The sauter mean diameter can be interpreted as the ratio of the total volume of the droplets in a spray to the droplets surface area; while the DeBrouckere diameter is the ratio of the square of the droplet surface area to the droplet volume. Consequently, if the two ratios, discussed above, for a single droplet are identical to those of a spray of droplets, the ratio A_i/A calculated for a single droplet can be applied to the spray described by distribution function.

Finally, the fraction of maximum area of influence is represented in terms of the droplet mass per unit area, $(w_s \Delta t)$, the initial surface temperature, T_s and the mean diameters $\bar{D}_{32}$ and $\bar{D}_{43}$. The mean diameters can be calculated by using various droplet size distribution functions which represent different types of sprays.

For the purpose of fire extinguishment, it is desirable to determine the minimum droplet mass necessary for cooling the hot surface, i.e., $(w_s \Delta t)_{min}$. In order to evaluate it, a criteria is needed to determine whether or not the hot surface is cooled. The proposed criteria is that the fraction of maximum area of influence is at least larger than 1.0, i.e.,

$$\frac{A_i}{A} \geq \epsilon \ , \qquad \text{where} \qquad \epsilon \geq 1 \qquad (4.20)$$

Note that ϵ is a cooling index which indicates whether or not the hot surface is cooled. It is at least larger than 1.0, however, it should be determined by experiment. This cooling index is in principle similar to the

flooding index proposed by Rizza [6]. Furtherfore, the time interval Δt must be related to the average droplet cooling effect duration. The results of the solid thermal computation show that Δt can be set equal to twice the evaporation time of the average diameter droplet.

By applying the above criteria to Eq. (4.19), $(w_s \Delta t)_{min}$ can be calculated by the following equation:

$$(w_s \Delta t)_{min} \geq \epsilon \{ C(T_s) [\frac{0.092}{\bar{D}_{32}} + \bar{D}_{43} e^{(-0.05\ T_s)}] \}^{-1} \qquad (4.21)$$

Hence, the minimum droplet mass per unit area for cooling the hot surface, $(w_s \Delta t)_{min}$, is determined by the initial surface temperature, two different mean diameters and a cooling index. In the next section, some calculations are made to evaluate $(w_s \Delta t)_{min}$ for three droplet size distribution functions and for a range of initial surface temperatures, i.e., 75 to 100 °C.

4.3.2. Sample Calculation As noted in Section 4.3.1, $(w_s \Delta t)_{min}$ is evaluated for the Rosin-Rammler, the Nukiyama-Tanasawa and the Log-Probability distribution functions. A brief description concerning these distribution functions is given. Subsequently, their application to the multi-droplet model is presented.

An accurate understanding of droplet size distribution is fundamental for the analysis of the mass and heat transport. Because of its importance, numerous distribution functions have been proposed. The three functions

mentioned above represent three typical droplet size distributions of a spray which is considered as a system of liquid droplets in a continuous fluid phase. A critical examination of the droplet size distribution is referred to an excellent paper written by Mugelle and Evans [3].

A distribution function includes two essential concepts: a mean value and a measure of tne deviation from this mean. These two concepts are represented by the mean diameter $\bar{D}$ and the distribution parameter δ. By specifying proper $\bar{D}$ and δ, the distribution function can be used to predict the droplet size distribution in a spray. Subsequently, different order of mean diameters $\bar{D}_{qp}$ can be calculated from the distribution, for example, $\bar{D}_{32}$ and $\bar{D}_{43}$ which have been discussed in Section 4.3.1.

The Rosin-Rammler (R-R) distribution function is generally given in the cumulative volume form:

$$1 - v = e^{-(D/\bar{D})^{\delta}} \tag{4.22}$$

where $1 - v$ is the volume fraction of droplets having diameter larger than D. From Eq. (4.22), the volume distribution form can be obtained:

$$\frac{dv}{dD} = \frac{\delta\, D^{\delta-1}}{\bar{D}^{\delta}}\; e^{[-(D/\bar{D})^{\delta}]} \tag{4.23}$$

or in non-dimensional form:

$$\bar{D}\,\frac{dv}{dD} = \delta\, z^{\delta-1}\, e^{(-z^{\delta})} \tag{4.24}$$

where

$$z = D/\bar{D} \tag{4.25}$$

The Nukiyama-Tanasawa distribution (N-T) function is an empirical equation. The volume distribution form is given as:

$$\frac{dv}{dD} = \frac{\delta\, b^{6/\delta}}{\Gamma(6/\delta)}\, D^5\, e^{(-b\, D^{\delta})} \tag{4.26}$$

where b has the dimension of $D^{-\delta}$ and $\Gamma(6/\delta)$ is a gamma function of $6/\delta$. If b is taken as $\bar{D}^{(-\delta)}$, the N-T is represented by the following equation:

$$\frac{dv}{dD} = \frac{\delta\, \bar{D}^{(-6)}}{\Gamma(6/\delta)}\, D^5\, e^{-(D/\bar{D})^{\delta}} \tag{4.27}$$

or in non-dimensional form:

$$\bar{D}\,\frac{dv}{dD} = \frac{\delta\, z^5}{\Gamma(6/\delta)}\, e^{(-z^{\delta})} \tag{4.28}$$

The Log-Probability (L-P) distribution function assumes a 'normal distribution' of y value; i.e.,

$$\frac{dv}{dy} = \frac{\delta}{\sqrt{\pi}}\, e^{(-\delta^2 y^2)} \tag{4.29}$$

where y is defined as the natural logarithmic value of z; that is,

$$y = \ln z = \ln(D/\bar{D}) \tag{4.30}$$

In non-dimensional form is given as:

$$\bar{D}\,\frac{dv}{dD} = \frac{\delta}{\sqrt{\pi}\,z}\; e^{[-\delta^2(\ln z)^2]} \qquad (4.31)$$

Figures 20 through 22 illustrate the R-R, N-T and L-P distribution functions for three δ values (i.e., δ = 2, 3, 4). In these figures, the non-dimensional forms of the volume distributions are presented, Eqs. (24), (28) and (31). On the basis of these figures, two observations can be made:

1. When δ is lower, the droplet size is more evenly distributed. On the other hand, when δ is higher, the droplets in a spray tend to have the same size; that is, the width of the distribution curve is narrower.

2. The most probable non-dimensional size (z), i.e., z_{mp} varies with δ in each distribution. Table 5 lists z_{mp} for the three distribution functions.

The mean diameters of R-R, N-T & L-P can be evaluated by using Eq. (4.16). They are listed in Table 6 (see Ref. [2]).

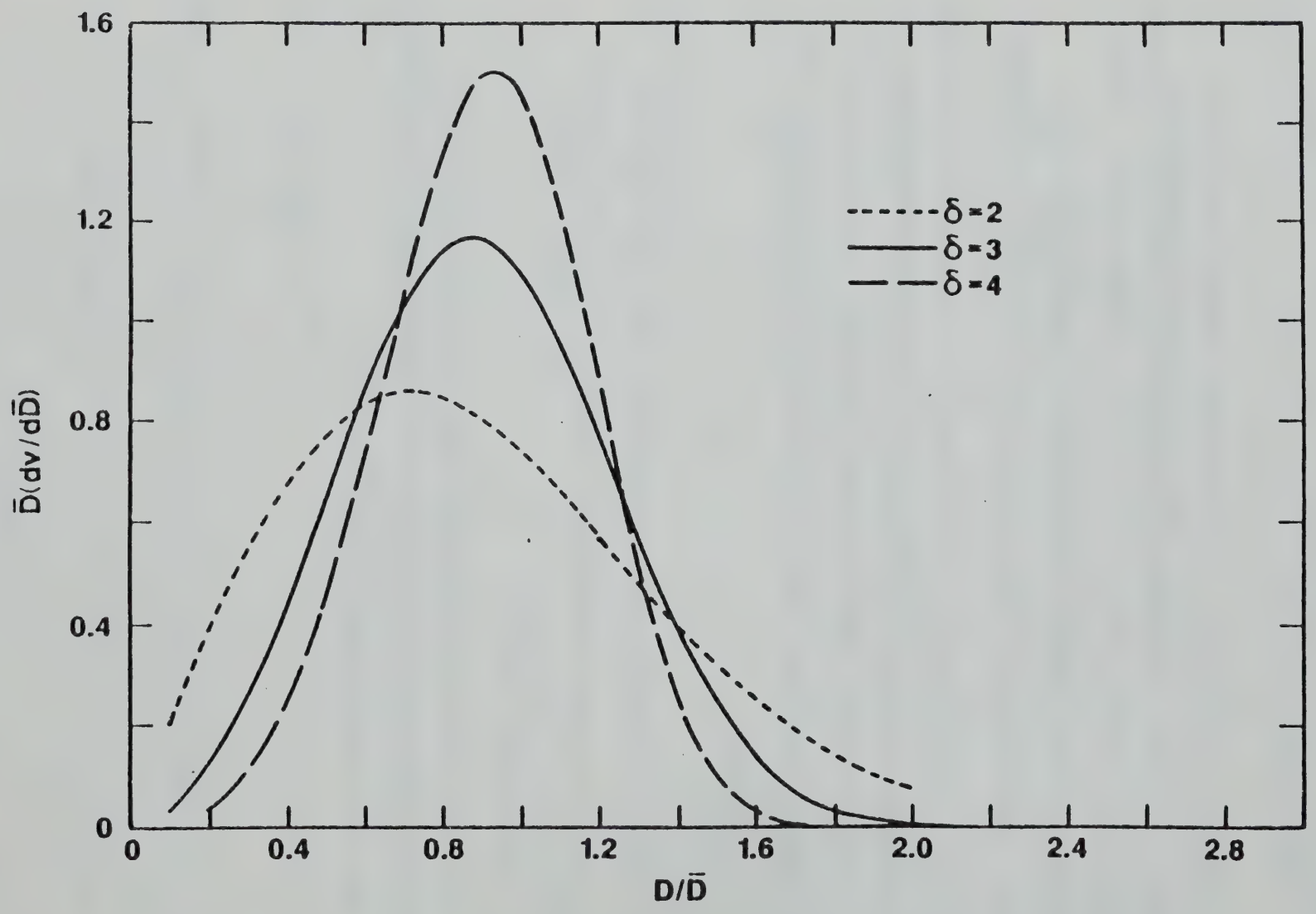

FIGURE 20. Rosin-Rammler Distribution

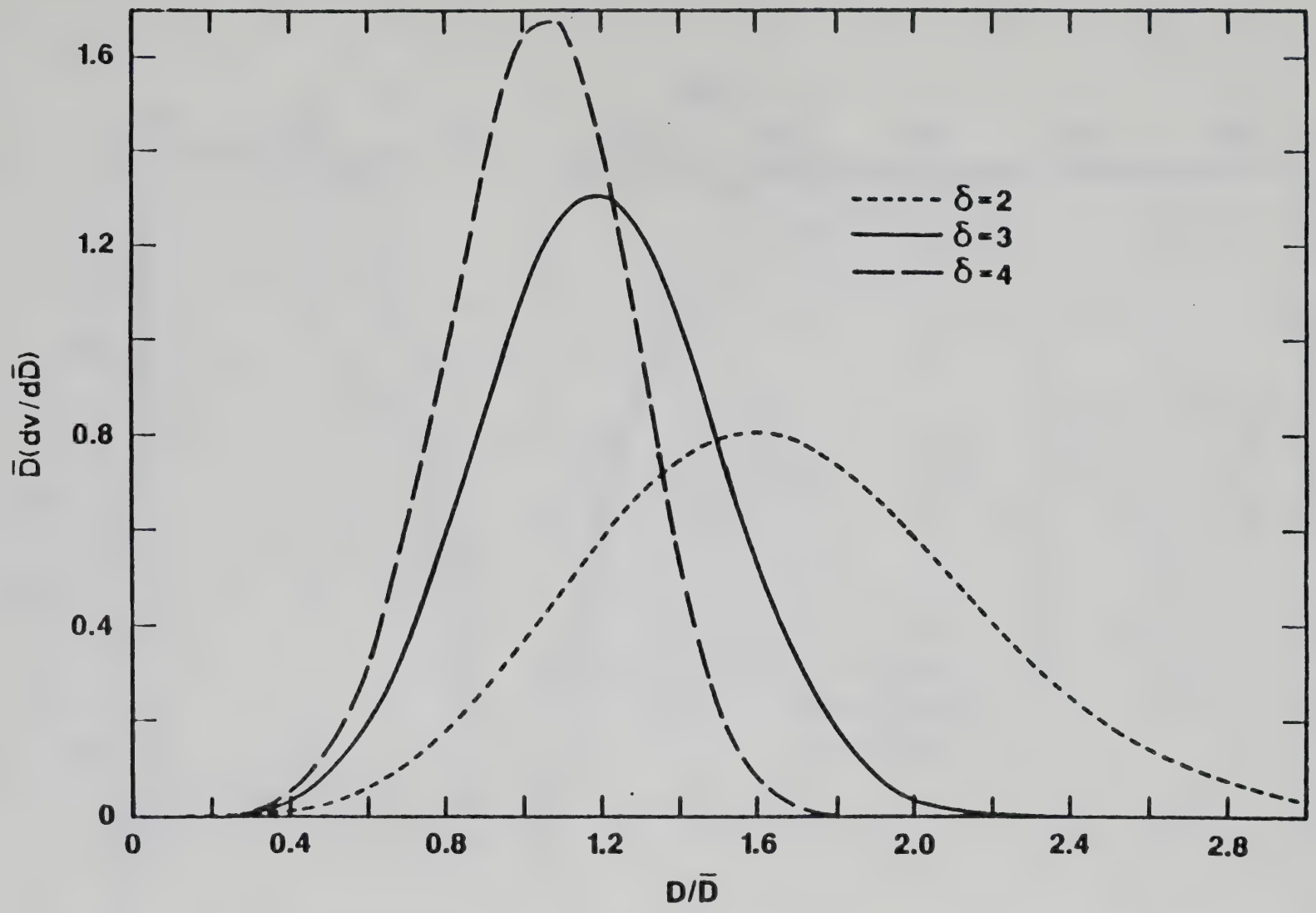

FIGURE 21. Nukiyama-Tanasawa Distribution

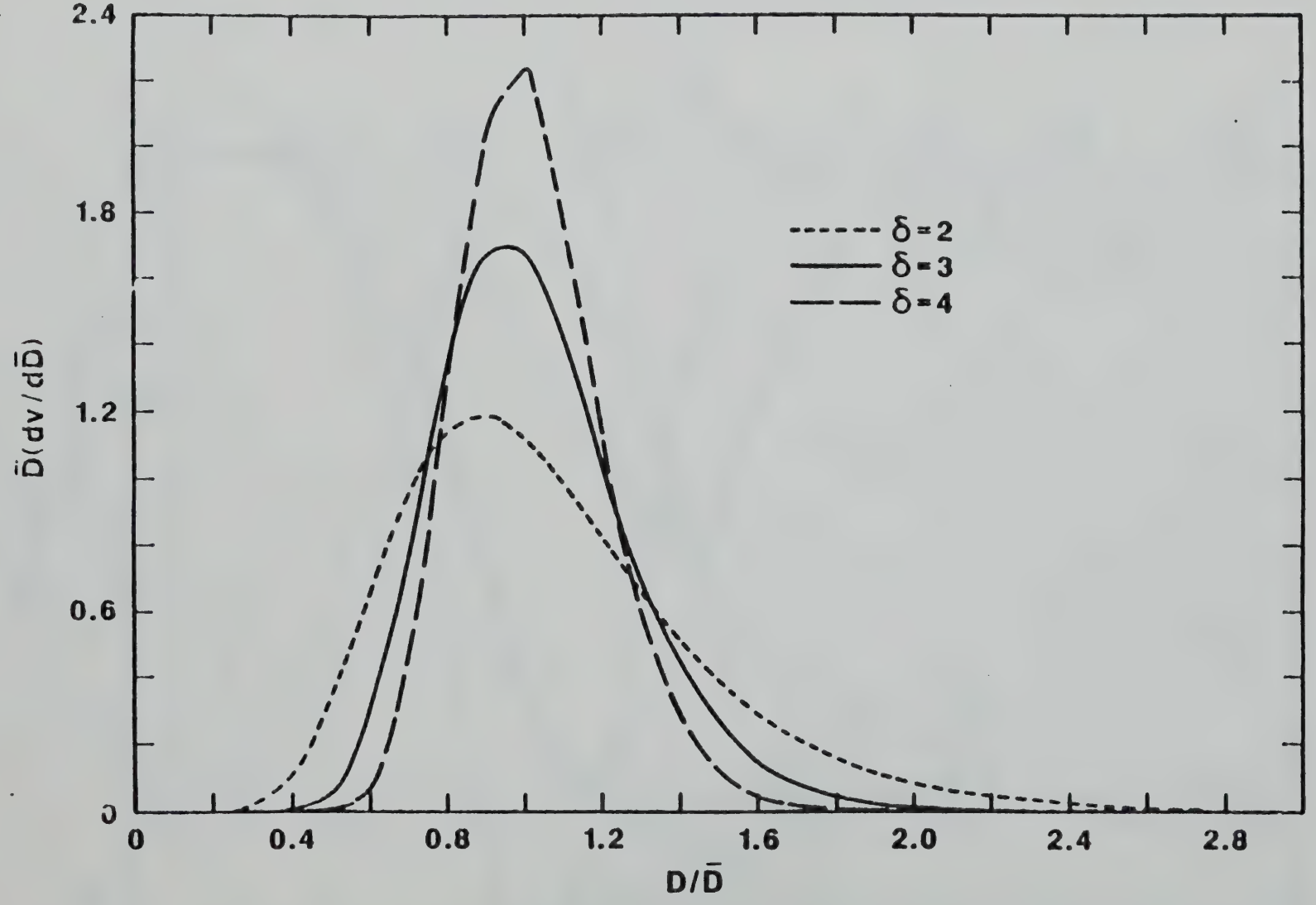

FIGURE 22. Log-probability Distribution

TABLE FIVE The Most Probable z_{mp}	
R-R	$\left(\frac{\delta-1}{\delta}\right)^{1/\delta}$
N-T	$\left(\frac{5}{\delta}\right)^{1/\delta}$
L-P	$e^{-(1/2\delta)^2}$.

TABLE SIX The Mean Diameter $\bar{D}_{qp}$	
R-R	$\bar{D}^{q-p}\left[\Gamma\left(\frac{q-3}{\delta}+1\right)\right] / \left[\Gamma\left(\frac{p-3}{\delta}+1\right)\right]$
N-T	$\bar{D}^{q-p}\left[\Gamma\left(\frac{q+3}{\delta}\right)\right] / \left[\Gamma\left(\frac{p+3}{\delta}\right)\right]$
L-P	$\bar{D}\, e^{-(p+q-6)^2 / (4\delta^2)}$

Therefore, $\bar{D}_{32}$ and $\bar{D}_{43}$ can be calculated by using the equations given in Table 6. They are presented in Table 7.

TABLE SEVEN

$\bar{D}_{32}$ and $\bar{D}_{43}$

	$\bar{D}_{32}$	$\bar{D}_{43}$
R-R	$\bar{D}/[\Gamma(1 - 1/\delta)]$	$\bar{D}\ \Gamma(1 + 1/\delta)$
N-T	$\bar{D}\ [\Gamma(6/\delta)]/[\Gamma(5/\delta)]$	$\bar{D}\ [\Gamma(7/\delta)]/[\Gamma(6/\delta)]$
L-P	$\bar{D}\ e^{-1/(4\delta^2)}$	$\bar{D}\ e^{1/(4\delta^2)}$

In order to perform meaningful calculations by using the distribution functions, proper $\bar{D}$ and δ have to be used.

First, the criteria determining δ is that the $D/\bar{D}$ range of the distribution function should be smaller than the single droplet experimental range. In the experiment, the droplet diameter ranges from 0.8 to 4.5 mm; i.e.,

$$0.8 < D < 4.5 \text{ mm} \tag{4.32}$$

$$0.3 < D/\bar{D} < 1.7 \tag{4.33}$$

$$\bar{D} = (0.8 + 4.5)/2 = 2.65 \text{ mm} \tag{4.34}$$

Consequently, only the $\delta = 4$ curves for the three functions meet this criteria. Figure 23 illustrates three $\delta = 4$ curves. In order to compare them, the curves are shifted such that the most probable z, $(D/\bar{D})_{mp}$,

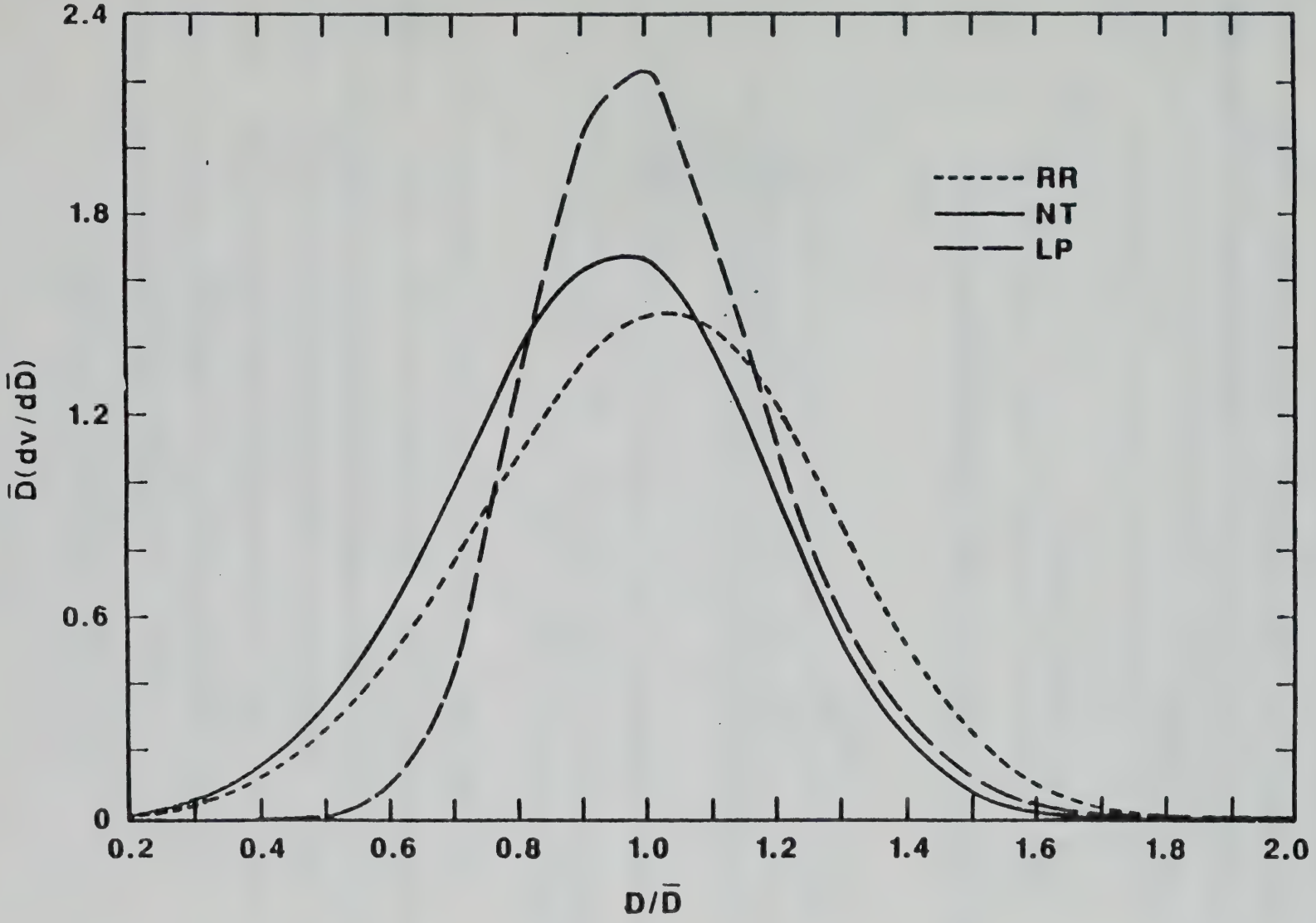

FIGURE 23. Distribution Comparison (δ-4)

is equal to 1.0. The three curves show similar behavior.

The determination of $\bar{D}$ is such that the most probable droplet diameter (D_{mp}) is the same for the three functions. The most probable diameter is taken as the average of the smallest (0.8 mm) and the largest (4.5 mm) droplet diameter in the experiment; i.e.,

$$D_{mp} = (0.8 + 4.5)/2 = 2.65 \text{ mm} \tag{4.35}$$

Therefore, $\bar{D}$ can be determined by the following equation:

$$\bar{D} = D_{mp} (D/\bar{D})_{mp} \tag{4.36}$$

where $(D/\bar{D})_{mp}$ is given in Table 5 for the three distribution functions.

By using the values of $\bar{D}$ and the equations presented in Table 7, $\bar{D}_{32}$ and $\bar{D}_{43}$ are calculated. Table 8 gives $\bar{D}$ as well as $\bar{D}_{32}$ and $\bar{D}_{43}$ for the three distribution function with $\delta = 4$.

TABLE EIGHT

The values of $\bar{D}$, $\bar{D}_{32}$ and $\bar{D}_{43}$

(mm)	$\bar{D}$	$\bar{D}_{32}$	$\bar{D}_{43}$
R – R	2.85	2.35	2.58
N – T	2.5	2.44	2.59
L – P	2.73	2.69	2.78

Finally, by substituting the values of $\bar{D}$, $\bar{D}_{32}$ and $\bar{D}_{43}$ into Eq. (4.21), the minimum droplet mass per unit area needed for cooling the hot aluminum surface $(w_s \Delta t)_{min}$ can be evaluated. Figure 24 illustrates three $(w_s \Delta t)_{min}$ curves for three distribution functions. Note that in this figure $(w_s \Delta t)_{min}$ is calculated by using the smallest cooling index; i.e., $\epsilon = 1.0$. On the basis of this figure, three conclusions can be drawn:

1. When the initial surface temperature increases, $(w_s \Delta t)_{min}$ increases. This implies more water is needed to cool the hotter surface.

2. The three distribution functions give similar distribution. This is reasonable, since the three distribution curves ($\delta = 4$) given in Figure 13 are similar though their functions are different.

3. The predicted $(w_s \Delta t)_{min}$ are in the range of 0.16 to 0.21 kg/m^2.

The conclusions discussed above are consistent and physically reasonable. However, the predicted $(w_s \Delta t)_{min}$ needs to be verified by the multi-droplet experiment. It should be noted that the predicted value is obtained by assuming that ϵ is equal to 1.0, i.e., $\epsilon = 1.0$. However, the cooling index ϵ should be determined experimentally. The value of the time integral Δt should be evaluated as twice the evaporation time of the most probable diameter droplet ($D_{mp} = 2.65$ mm).

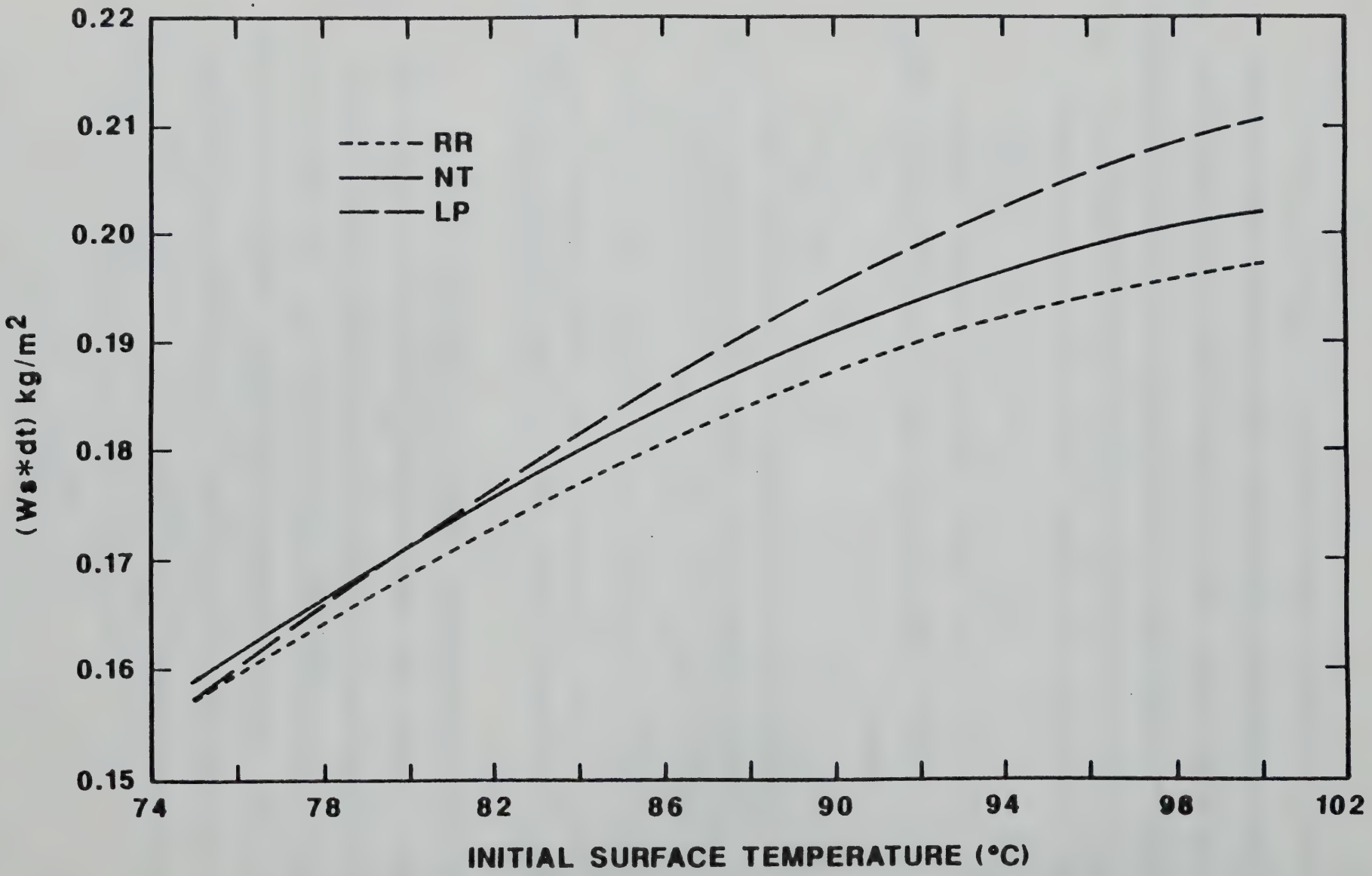

FIGURE 24. Minimum Water Mass Versus Initial Surface Temperature

4.4 Nomenclature

A	total surface area
A_d	area of droplet after deposit
A_D	area of droplet before deposit
A_i	maximum area of influence
ΔA_i	maximum area of influence induced by a droplet
$\Delta(\Delta A_i)$	maximum area of influence induced by a droplet
b	a parameter in the Nukiyama-Tanasawa Function
$C(T_i)$	a coefficient in Eq.(4.11)
d	droplet diameter after deposit
D	droplet diameter before deposit
D_m	the largest droplet diameter in a spray
D_{mp}	the most probable droplet diameter in a spray
D_o	the smallest droplet diameter in a spray
D	a mean droplet diameter
D_{qp}	mean droplet diameter with an order of p+q
D_{32}	sauter mean diameter
D_{43}	DeBrouckere diameter
$\Delta(\Delta m)$	mass of droplets having diameter between D and D+ΔD that reach the surface between t and t+Δt
L-P	Log-probability distribution function
m_d	mass of a droplet
Δn	number fraction of droplets having diameter between D and D+ΔD
N-T	Nukiyama-Tanasawa distribution function
p	an order index of mean diameter

q	an order index of mean diameter
r_d	maximum radius of a droplet after deposit
r_i	maximum radius of influence
R-R	Rosin-Rammler distribution function
t	time
Δt	twice the evaporation time of the most probable diameter droplet
T_s	initial surface temperature
Δv	volume fraction of droplets having diameter between D and D+ΔD
V	initial volume of droplet
V_i	maximum volume of influence
W_s	mass flow rate of droplets depositing on surface
w_s	mass flux of droplets depositing on surface
$(w_s \Delta t)_{min}$	minimum droplet mass per unit surface for cooling hot surface
y	a variable
z	non-dimensional parameter
z_{mp}	the most probable
ϵ	a cooling index
ρ_d	density of the droplet
τ	evaporation time of droplet
δ	distribution parameter
Γ	gamma function

5. REPORTING ACTIVITIES

The documents describing the research activities, published during the reporting period, are listed hereafter.

5.1 Internal Reports

M. di Marzo, A. K. Trehan, "Transient Cooling of a Hot Surface by Droplet Evaporation", NBS-GCR-86-516, 1986

M. di Marzo, D. D. Evans, "Evaporation of a Water Droplet Deposited on A hot High Thermal Conductivity Solid Surface", NBSIR 86-3384, 1986

M. di Marzo, D. D. Evans, A. K. Trehan, "The Cooling Effect of a Single Droplet on a Hot Semi-Infinite Metal Body", NBSIR 87-3517, 1987

5.2 Presentations

Annual Conference of the Center for Fire Research (NBS Gaithersburg, October 1986):

M. di Marzo, "The Cooling Effect of a Single Evaporating Droplet on a Hot Semi-Infinite Metal Body"

Eastern Session of the Combustion Institute (Puerto Rico, December 1986):

M. di Marzo, D. D. Evans, "The Cooling Effect of a Single Evaporating Droplet on a Hot Semi-Infinite Metal Body"

5.3 Publications

M. di Marzo, D. D. Evans, "Dropwise Evaporative Cooling of High Thermal Conductivity Materials", Heat and Technology, Vol. 5, No. 1-2, pp. 126-136, 1987

M. di Marzo, D. D. Evans, A. K. Trehan, "The Cooling Effect of a Single Evaporating Droplet on a Semi-Infinite Metal Body", Accepted for presentation at the ASME/JSME Joint Thermal Conference, Honolulu, 1987

M. di Marzo, D. D. Evans, "Evaporation of a Water Droplet Deposited on a Hot High Conductivity Solid Surface", Accepted for presentation at the 24th ASME/AIChE/ANS National Heat Transfer Conference, Pittsburgh, 1987

6. SUMMARY AND PERSPECTIVES

6.1 Low Conductivity Solid

The experimental results shown in the previous section are in all similar to the results obtained for aluminum. A notable difference is in the behavior of the shape parameter β_o. The data for aluminum indicated an upward trend of this parameter with rising temperatures, while, for the Macor, the data seem to show a constant value of about 1.42 (+/- 0.09).

The results of the code for the coupled liquid solid boundary will give some important indication concerning the radial temperature gradients at the liquid-solid interface. Furthermore, the code will also validate the assumption of uniform temperature under the droplet used for the high thermal conductivity solid (see also Seki [2]).

6.2 Radiation

Upon successfully demonstrate the capability of the code to predict the droplet-solid interaction, the more complex situation where the major heat source is radiant in nature can be addressed. In a typical fire application, the heat is radiated from the flames to the exposed solid surfaces. The droplet impinging on such surfaces will receive radiant heat from above as well as heat from below conducted through the solid. In order to analyze this situation, the solid-liquid model will be upgraded to incorporate the radiative heat transfer component. The numerical solution to this complex problem will be validated with adequate experimental measures. Both the radiative model and experiments will be performed in the second portion of the next grant period (1987-88). The results of this investigation will be

hopefully collapsed in simple area (volume) of influence relationships similar to those derived for the simple aluminum case.

6.3 Spray Cooling

The long term objective of this research program is to obtain a reliable model for solid fuel fire extinguishment. The results of the radiative model and experimentation will provide the basic information to derive a prediction of the cooling effect of a multi-droplet array. The methodology to extend the single droplet results to a droplet array is outlined. Validation of these predictions could be then derived from spray cooling measurements in actual fire environment.

The correct prediction of the cooling induced by a spray on solid surfaces exposed to fire will constitute a preliminary milestone in the study of the complex problem of solid fuel fire suppression.

7. REFERENCES

[1] M. diMarzo and A.K. Trehan, 'Transient Cooling of A Hot Surface By Droplets Evaporation', National Bureau of Standards Interagency Report, NBS-GCR-86-516, July 1986.

[2] M. Seki, H. Kawamura, K. Sanokawa, "Transient Temperature Profile of a Hot Wall Due to an Impinging Liquid Droplet", Journal of Heat Transfer (Transaction ASME), Vol. 100, pp. 176, 1978.

[3] R. A. Mugele and H. D. Evans, 'Droplet Size Distribution in Sprays', Industrial and Engineering Chemistry, Vol. 43, no. 6, June 1951, pp 1317-1324.

[4] C. Bonacina, S. Del Giudice and G. Comini, 'Dropwise Evaporation', Journal of Heat Transfer, Transaction ASME, Vol. 101, August 1979, pp 441-446.

[5] H. C. Lewis, D. G. Edwards, M. J. Goglia, R. I. Rice, L. W. Smith, 'Atomization of Liquids in High Velocity Gas Stream', Industrial and Engineering Chemistry, Vol. 40, No. 1, January 1948, pp 67-74.

[6] J. J. Rizza, 'A Numerical Solution to Dropwise Evaporation', Journal of Heat Transfer, Transaction ASME, Vol. 103, August 1081, pp 501-507.

FORM NBS-114A (REV.11-84)

U.S. DEPT. OF COMM. **BIBLIOGRAPHIC DATA SHEET** (See instructions)	1. PUBLICATION OR REPORT NO. NBS/GCR-87/534	2. Performing Organ. Report No.	3. Publication Date November 1987

4. TITLE AND SUBTITLE

Transient Cooling of a Hot Surface by Droplets Evaporation

5. AUTHOR(S)

M. di Marzo, Z.Y. Wang, W.H. Meng

6. PERFORMING ORGANIZATION (If joint or other than NBS, see instructions)

University of Maryland
Mechanical Engineering Dept.
College Park, MD

7. Contract/Grant No.
Grant 70NANB5H0525

8. Type of Report & Period Covered
March 1986-March 1987

9. SPONSORING ORGANIZATION NAME AND COMPLETE ADDRESS (Street, City, State, ZIP)

National Bureau of Standards
Department of Commerce
Gaithersburg, MD 20899

10. SUPPLEMENTARY NOTES

☐ Document describes a computer program; SF-185, FIPS Software Summary, is attached.

11. ABSTRACT (A 200-word or less factual summary of most significant information. If document includes a significant bibliography or literature survey, mention it here)

This report describes the research performed during the period March 1986-March 1987 under a joint research program between the Mechanical Engineering Department of the University of Maryland and the Center for Fire Research of the National Bureau of Standards. The research is conducted in the laboratories of the CFR by a Graduate Research Assistant of the ME Department under the joint supervision of Dr. Marino di Marzo (ME Dept.-UMCP) and of Dr. David D. Evans (CFR - NBS). The study of droplet evaporation on a high thermal conductivity semi-infinite solid is investigated as well as the solid thermal behavior both theoretically and experimentally. The behavior of a low thermal conductivity solid is the objective of experimental studies. A coupled analytical model for the solid and the evaporating liquid is being derived to predict the cooling effect induced by the evaporating droplet. The results of the analytical model will be available in the Summer 1987. In parallel with the single droplet study, a preliminary modelling effort is initiated to characterize the cooling effect of a multi-droplet array. Typical spray distributions are used to derive some information on overall cooling effect of a hot surface. A summary of the presentations and of the publications produced during the reporting period is also enclosed. A brief outline of the future research activities is given in the end of this report to provide a (prospective) of the reported results in the framework of the overall research program.

12. KEY WORDS (Six to twelve entries; alphabetical order; capitalize only proper names; and separate key words by semicolons)

13. AVAILABILITY

☒ Unlimited
☐ For Official Distribution. Do Not Release to NTIS
☐ Order From Superintendent of Documents, U.S. Government Printing Office, Washington, DC 20402.
☒ Order From National Technical Information Service (NTIS), Springfield, VA 22161

14. NO. OF PRINTED PAGES
77

15. Price
$13.95